6-24-2022 10:00 AM

The role of reactive oxygen species in the accumulation of driver mutations in B cell acute lymphoblastic leukemia

Mia P. Sams, *The University of Western Ontario*

Supervisor: DeKoter, Rodney P., *The University of Western Ontario*

A thesis submitted in partial fulfillment of the requirements for the Master of Science degree in Microbiology and Immunology

Abstract

B cell acute lymphoblastic leukemia (B-ALL) is the most prevalent type of cancer in young children and is associated with recurrent mutations and high levels of reactive oxygen species (ROS). The antioxidant N-acetylcysteine was tested for its ability to prolong lifespan of a mouse model of B-ALL and reduce frequency of mutations. Mice treated with 1g/L of N-acetylcysteine in drinking water were found to have delayed onset of B-ALL at 11 weeks of age and changes in gene expression relating to B cell development, calcium-apoptosis signaling, and pathways in cancer, although no differences in lifespan were observed. Tumours from treated mice had 100% incidence of pseudokinase domain mutations in *Jak1* or *Jak3*. These results indicate that tumours in treated mice develop later in life but become more aggressive than control tumours and that JAK mutations may act as drivers of leukemogenesis in the presence of lower levels of ROS.

Keywords

B cell acute lymphoblastic leukemia, B cells, leukemia, cancer, reactive oxygen species, antioxidants, N-acetylcyteine, Janus kinase, driver mutations, immunology, mouse model, calcium signaling

Summary for Lay Audience

B cell acute lymphoblastic leukemia (B-ALL) is the most prevalent cancer occurring in young children and remains a leading cause of childhood death. B-ALL is associated with mutations in genes that are necessary for the development of B cells as well as high levels of reactive oxygen species (ROS). ROS are highly reactive molecules that can be blocked by chemicals known as antioxidants. High levels of ROS in cells can cause mutations in DNA, so we tested the ability of the antioxidant N-acetylcysteine for its ability to reduce the frequency of mutations in a mouse model of B-ALL. We found that treatment of mice with N-acetylcysteine did not increase survival of our mice, but that it did significantly change the biology of the tumours that formed. Tumours in treated mice started developing later in life compared to control mice and had differences in the level of expression of genes that are involved in B cell development, regulation of cell death, and cancer. Since tumours in treated mice started developing later in life, but still resulted in death at the same time as control mice, the tumours in treated mice may be more aggressive once they do develop. Analysis of the mutations in these tumours suggested that mutations in *Jak* genes may be necessary for the development of leukemia in treated mice, as they were found in 100% of the treated tumours. In conclusion, we have shown that N-acetylcysteine can delay the development of leukemia, but that it cannot prevent it.

Co-Authorship Statement

The experiments in the following thesis were designed by Dr. Rodney P. DeKoter and Mia Sams, with input from Dr. Steven M. Kerfoot and Dr. Sung O. Kim. All experiments were performed by Mia Sams. This thesis was written by Mia Sams and reviewed by Dr. Rodney P. DeKoter and Dr. Steven M. Kerfoot.

Acknowledgments

First and foremost I would like to thank my family for supporting me in every endeavour and for being so excited to hear about my research every time I visited home and over Zoom throughout the pandemic. Without your ongoing encouragement, not only though my Master's degree, but in life, I would not be where I am today.

I would also like to wholeheartedly thank my supervisor Dr. Rodney DeKoter for his kind mentorship over the last two years, from his guidance through the depths of troubleshooting (of which there was a lot) to sharing in the excitements of new discoveries. Thank you for the wonderful opportunity to experiment with this research in my own way while providing all the support I needed.

Thank you to my advisory committee members Dr. Steven Kerfoot and Dr. Sung Kim for providing me with valuable feedback and ideas for moving my project onward to greater things!

Thank you to all members of the DeKoter lab over the past years for making the lab such an enjoyable place to be, and for the friendships maintained outside the lab with fun events like our annual outdoor pumpkin carving fiascos. Thank you especially to Hannah who was willing to answer every silly question I had as a new member of the lab and who is now a lifelong friend. Thank you to Bruno for his generous assistance in bioinformatics and RNA sequencing, as well as Sherry for helping me take some much-needed weekends off by monitoring my mice.

I am especially grateful for the friends who made the past two years so enjoyable in the midst of work and lockdowns. Nicholas, Dylan, and Graeden, thank you for the late nights, the many laughs, and unforgettable memories (and maybe some permanent injuries). Colleen and Jacob, thank you for the love and support that only fellow graduate students can provide in times of strife. Hannah, Patrick, and Frank, thank you for giving me an escape from school to wind down whether it be watching Marvel movies, eating good food, or struggling to survive a camping trip.

Thank you to Jodi Dutz and the SAR team for assisting me in providing the best possible animal care throughout my studies and Kristin Chadwick for always being willing to help me learn flow cytometry.

The number of people who have made my Master’s an unforgettable experience is immeasurable and I cannot thank everyone enough for their love and support.

Table of Contents

Abstract ii

Summary for Lay Audience iii

Co-Authorship Statement iv

Acknowledgments v

Table of Contents vii

List of Tables x

List of Figures xi

Chapter 1 1

1 Introduction 1

1.1 B cell development 1

1.2 Transcription factor regulation of B cell development 4

1.3 E26 transformation-specific family of transcription factors PU.1 and SpiB 7

1.4 B cell acute lymphoblastic leukemia 8

1.5 Mechanisms of mutagenesis and repair 9

1.6 The role of reactive oxygen species in leukemogenesis 10

1.7 The use of N-acetylcysteine as a therapeutic 11

1.8 Two mechanisms of mutation accumulation in Mb1-CreΔPB mice 13

1.9 Research rationale and central hypothesis 14

Chapter 2 15

2 Materials and Methods 15

2.1 Breeding of mice 15

2.2 Mouse genotyping 15

2.3 Water preparation 15

2.4 Water administration schedule 15

2.5 Tissue extraction and flow cytometry 17

2.6 RNA sequencing 17

2.7 Pathway analysis 17

2.8 Statistical analysis 20

Chapter 3 21

3 Results 21

3.1 Administration of 1g/L N-Acetylcysteine in water did not confer a survival advantage to Mb1-CreΔPB mice compared to control water 21

3.2 Female mice weigh significantly less than male mice, and therefore receive a higher NAC dose per body weight 28

3.3 Female mice that weighed less tended to survive longer when treated with 1g/L NAC 31

3.4 Mice within the same litter tend to develop leukemia at a similar timepoint compared to non-littermates 33

3.5 Administration of 1g/L of N-acetylcysteine resulted in delayed tumour growth at 11 weeks of age 35

3.6 Mice with low CD19 positivity have lower thymus cell count to thymus weight ratios 42

3.7 6.5g/L NAC water does not confer a survival advantage 44

3.8 Leukemias from mice on NAC and control water have significant differences in gene expression 49

3.9 Genes involved in somatic hypermutation and class-switch recombination of the B cell receptor are differently expressed between treatment and control mice 60

3.10 Leukemic mice have high mutation frequency in Ikzf3, Jak1, Jak3, Trp53, and Sf3b1 62

Chapter 4 66

4 Discussion 66

4.1 Differences in dose per gram of body weight affected survival of Mb1-CreΔPB mice receiving 1g/L N-acetylcysteine 66

4.2 Leukemia progression occurs rapidly and may be postponed, but accelerated by N-acetylcysteine administration 67

4.3 Wider variation in gene expression in control mice may be due to accumulation of driver mutations late in clonal evolution 69

4.4 Evidence for physiological differences between cells in N-acetylcysteine and control mouse thymuses 70

4.5 Calcium signaling for apoptosis is a candidate pathway affected by NAC treatment 71

4.6 Mutations in Janus Kinases and Ikzf3 may act as driver mutations of leukemogenesis 72

4.7 Conclusion and hypothetical model 74

4.8 Future directions 77

References 79

Curriculum Vitae 86

List of Tables

Table 1. Primer pair used for amplification of the *Cre* gene in Mb1-CreΔPB mouse genotyping samples. 16

Table 2. Characteristics of all mice on the 1g/L N-acetylcysteine water trial ordered by experimental group and date of birth. 23

Table 3. Characteristics of all mice on the 11-week N-acetylcysteine water trial. 37

Table 4. Characteristics of all mice on the 6.5g/L N-acetylcysteine water trial. 46

List of Figures

Figure 1. Simplified schematic of the stages of B cell development with focus on the Pro-B to immature B cell stages. 3

Figure 2. Overview of the JAK/STAT pathway as activated by interleukin-7 binding to its receptor. 6

Figure 3. Chemical structures of N-acetylcysteine (right) and its amino acid derivative, L-cysteine (left). 12

Figure 4. Treatment schedules for mice on NAC water studies. 18

Figure 5. Workflow for the post-processing and analysis of RNA sequencing data. 19

Figure 6. Mice administered 1g/L of N-acetylcysteine through drinking water did not display an increase in survival compared to mice fed control water. 24

Figure 7. Mice administered 1g/L of N-acetylcysteine through drinking water displayed differences in survival between sexes, but no difference in survival compared to control mice. 26

Figure 8. There is no significant difference in thymus CD19 positivity, thymus weight, or thymus cell count in sick mice between the N-acetylcysteine treatment and control groups. 27

Figure 9. Averaged mouse weights split by treatment group and sex. 29

Figure 10. Adult female mice weigh on average significantly less than adult male mice..... 30

Figure 11. Female mice on NAC that weigh less survive longer, whereas female control mice have no difference in weight based on survival. 32

Figure 12. Mb1-CreΔPB mice from the same litter tend to develop leukemia at similar time points. 34

Figure 13. Mb1-CreΔPB mice treated with 1g/L NAC had significantly lower CD19 positivity, indicating lower B cell infiltration into their thymuses while thymus weight and cell counts were not significantly different. 38

Figure 14. Four Mb1-CreΔPB mice from the same litter split into treatment and control water groups displayed significant differences in thymic CD19 positivity, weight, and cell count after 11 weeks. 39

Figure 15. Thymuses extracted from control mice tended to be redder in colour compared to thymuses from mice receiving NAC at the 11-week timepoint. 40

Figure 16. Mice treated with 1g/L NAC have significantly higher expression of vasculature marker gene *Pecam1*. 41

Figure 17. Mice with lower B cell infiltration into the thymus have lower thymus cell count to thymus weight ratios. 43

Figure 18. Male and female mouse weights averaged over time. 45

Figure 19. Mice administered 6.5 g/L of NAC through drinking water did not display an increase in survival compared to mice fed control water. 47

Figure 20. 6.5g/L NAC-treated mice have significantly lighter thymuses at time of euthanasia compared to control mice, whereas there is no significant difference in thymus CD19 positivity or thymus cell count. 48

Figure 21. Principal component evaluation of differential expression analysis of Mb1-CreΔPB tumours. 51

Figure 22. Heatmap of the top 50 features of each treatment group in terms of expression. . 52

Figure 23. DAVID pathway analysis of the KEGG gene-set “Pathways in Cancer”. 53

Figure 24. DAVID pathway analysis of the KEGG gene-set “Calcium Signaling Pathway”. 54

Figure 25. DAVID pathway analysis of the KEGG gene-set “T cell Receptor Signaling Pathway”. 55

Figure 26. The effect of NAC on expression genes involved in T cell activation in Mb1-CreΔPB mice..... 56

Figure 27. The effect of NAC on expression of genes involved in calcium regulation of apoptotic signals in the endoplasmic reticulum and mitochondria in Mb1-CreΔPB mice..... 58

Figure 28. Simplified schematic of the proposed calcium signaling pathway affected by NAC treatment. 59

Figure 29. Gene expression of *Aicda* and *Rag1/2* in NAC-treated and control mice..... 61

Figure 30. A representative screenshot of the IGV output for the *Jak3* R653H mutation. 63

Figure 31. Identified mutations in conserved regions of Jak1, Jak3, Ikzf3, Trp53, and Sf3b1 genes. 65

Figure 32. A working model of the process of 1g/L NAC delaying but streamlining leukemogenesis. 76

Chapter 1

1 Introduction

B cell acute lymphoblastic leukemia (B-ALL) is the most common cancer in young children and despite high remission rates, still represents a leading cause of childhood death (Iacobucci and Mullighan 2017). B cell neoplasms often originate from early stages of B cell development (Roberts and Mullighan 2015) and are associated with recurrent mutations in the genes that regulate this developmental process (Zhang *et al.* 2017).

1.1 B cell development

The mammalian immune system has evolved over millions of years to protect against foreign pathogens and cancerous cells. It is comprised of innate and adaptive immunity, the former of which consists of physical and chemical barriers, and cells such as macrophages, and natural killer cells that form the non-specific so called ‘first line of defense’ against invading pathogens. On the other hand, the adaptive immune system works in a highly specific manner and includes T and B lymphocytes that can mount an antigen-specific response, which in conjunction with innate immunity, works to clear bacterial, viral, or parasitic invasions.

B lymphocytes, or B cells, exert their most well-known function by producing and secreting antibodies specific to a wide variety of pathogens. B cells are also involved in many other immune functions including the induction of T cell immunity (Ron *et al.* 1981). B cells also secrete cytokines, and can act in either regulatory (regulatory B cells) or immune-inducing (effector B cells) manners depending on the cytokines they secrete. Regulatory B cells typically secrete IL-10 (Fillatreau *et al.* 2002), while effector B cells can secrete IL-2, IL-4, TNFα, and IFNγ, among others (Vasquez *et al.* 2015).

B cells develop from hematopoietic stem cells in the bone marrow which mature into lymphoid progenitor cells that at this stage either follow to the B or T cell lineage, depending on cytokine signaling. Lymphoid progenitors that begin development into the B cell lineage first develop into pre-pro-B cells. Once these cells transition to the pro-B

cell stage, they entirely commit to the B cell line through the process of variable (V), diversity (D), and joining (J) segments recombining within the Immunoglobulin Heavy (IgH) chain locus of the B cell receptor (BCR) (Brack *et al.* 1978). VDJ recombination, mediated by RAG-1/2 (Schatz, Oettinger, and Baltimore 1989) ultimately leads to the production and surface expression of the pre-BCR and transition to the large pre-B cell stage of development. Large pre-B cells generate clonal expansion before becoming small pre-B cells, which undergo a second rearrangement of the variable and joining regions in the Immunoglobulin Light (IgL) locus to become immature B cells with full ability to recognize antigen (Clark *et al.* 2014). Immature B cells undergo negative selection against those that recognize self-antigens and those that pass disperse to secondary lymphoid tissues including the spleen and lymph nodes where they develop into mature naïve B cells (Shlomchik and Weisel 2012). When a naïve B cell is presented with antigen, it becomes activated and localizes to the site of disease. A simplified schematic of B cell development is pictured in **Figure 1.**

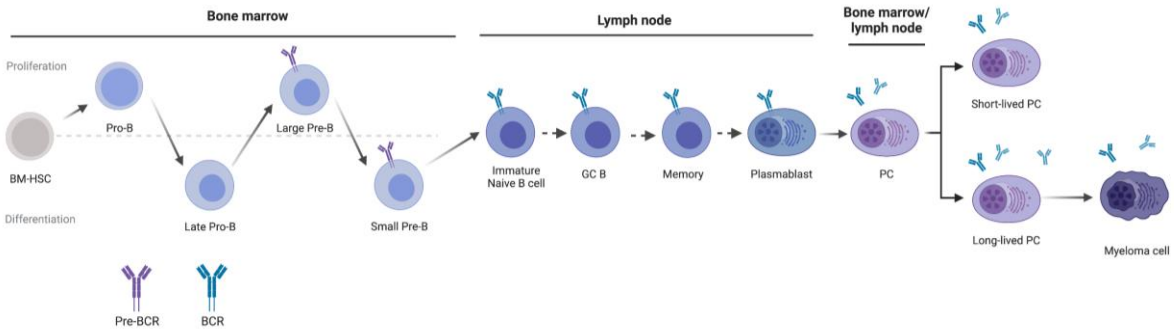

Figure 1. Simplified schematic of the stages of B cell development with focus on the Pro-B to immature B cell stages.

BM-HSC: hematopoietic stem cells located in the bone marrow. Pro-B: progenitor B cell, Pre-B: precursor B cell, GC B: germinal center B cell, PC: plasma cell, BCR: B cell receptor. Adapted from Clark *et al.* 2014.

1.2 Transcription factor regulation of B cell development

The development of B cells is a highly complex process that involves many changes in cell signaling and is regulated by a variety of transcription factors. From the stages of multipotent progenitors to pre-B cells, many transcription factors are involved in the progression of early B cells through development, some of the most important being PU.1 (encoded by *Spi1*), Ikaros (encoded by *Ikzf1*), E2A (encoded by *Tcfe2a*), EBF1 (encoded by *Ebf1*), Pax5 (encoded by *Pax5*), Aiolos (encoded by *Ikzf3*), Sox4 (encoded by *Sox4*), Lef1 (encoded by *Lef1*), Bcl11a (encoded by *Evi9*), and GABP (encoded by *Gabpa*) (Nutt and Kee 2007). A model of transcription factor involvement constructed by Nutt and Kee (2007) highlights the importance and interconnected nature of the actions of these 10 key transcription factors where they interact with each other to regulate gene expression necessary for the commitment, differentiation, and eventual clonal expansion of pre-B cells.

Additionally, the Janus Kinase (JAK) family of proteins is implicated in the development of B cells and includes *Jak1*, *Jak2*, *Jak3*, and *Tyk2*. JAK proteins are associated with cytokine receptors located on the plasma membrane of lymphoid progenitor cells (Scott 2013). Binding of a cytokine, such as IL-7, to its receptor causes autophosphorylation of its associated JAK, which proceeds to phosphorylate and activate signal transducer and activator of transcription (STAT) proteins which localize to the nucleus and act as transcription factors to increase expression of genes related to proliferation and cell survival (Ghoreschi, Laurence, and O'Shea 2009). Specifically, the IL-7/JAK1/3/STAT5 pathway (outlined in **Figure 2**) has been implicated in cancers of the B cell lineage, where gain-of-function mutations in *Jak1* or *Jak3* trigger constitutive activation of this pathway through increased levels of ROS generated through phosphorylated STAT5 (Bourgeais *et al.* 2017). Typically, the pseudokinase domain of JAK proteins is responsible for autoregulation of activation and prevents this constitutive activation (Saharinen and Silvennoinen 2002). Studies investigating patients with B-ALL with or without initiating chromosomal changes such as the commonly studied ETV6-RUNX1 or BCR-ABL1 gene fusions have identified consistent and recurring mutations within the

kinase and pseudokinase domains of JAK proteins, suggesting that the predicted overactivation of the JAK/STAT pathway contributes to leukemogenesis, potentially due to positive feedback between JAK/STAT signaling and ROS production (Mullighan *et al.* 2009, Lilljebjorn *et al.* 2012, Prieto-Bermejo *et al.* 2018).

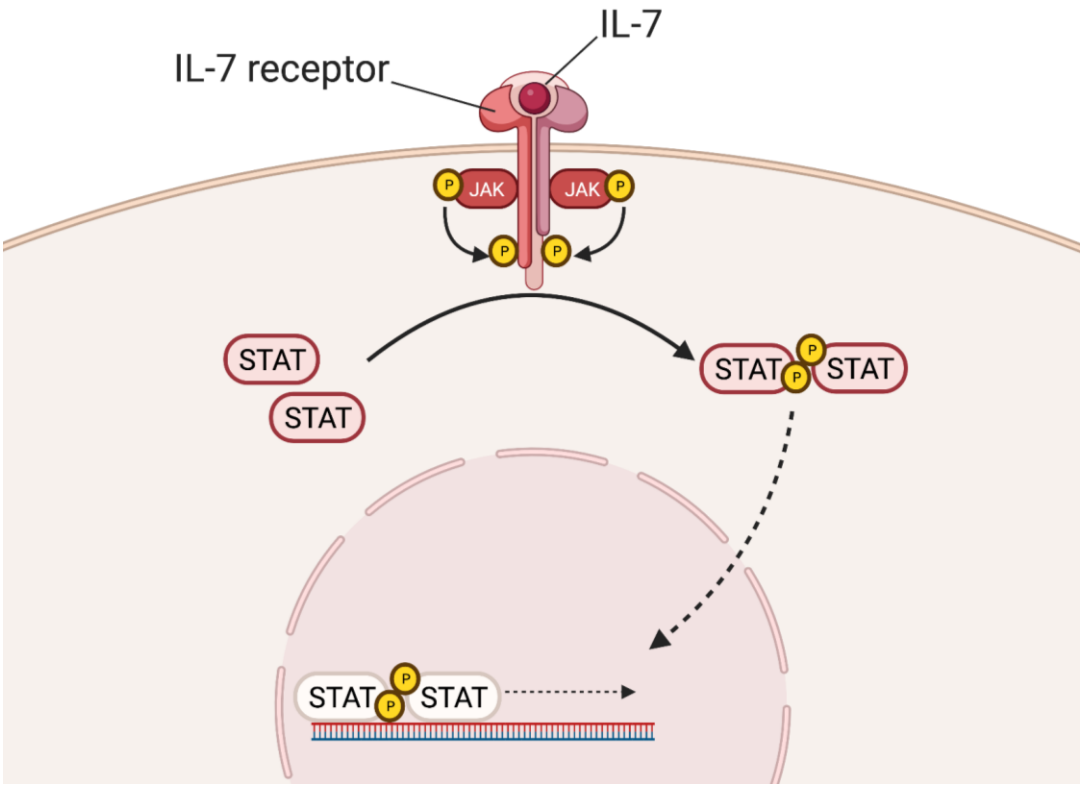

Figure 2. Overview of the JAK/STAT pathway as activated by interleukin-7 binding to its receptor.

When IL-7 binds to its receptor, JAK proteins associated with the intracellular side of the receptor autophosphorylate. The JAKs then phosphorylate the IL-7 receptor, allowing STAT5 to anchor the receptor, become phosphorylated, dimerize, and enter the nucleus to induce expression of genes involved in proliferation and cell survival.

1.3 E26 transformation-specific family of transcription factors PU.1 and SpiB

A specific family of transcription factors implicated in the intricate process of B cell development is the E26-transformation-specific (ETS) family of transcription factors, classified according to the presence of the sequence-specific ETS DNA-binding domain (Karim *et al.* 1990). Consisting of 85 amino acids, this domain interacts with and binds to a short DNA sequence including a GGAA/T motif (Nunn *et al.* 1983). ETS proteins are associated with diverse functions mostly related to the cell cycle, cell differentiation, and proliferation, all necessary during B cell development.

Within the *Spi* subfamily of ETS transcription factors, SpiB (encoded by *Spib*) and PU.1 (encoded by *Spi1*) activate the transcription of genes promoting B cell development (Solomon *et al.* 2015, Xu *et al.* 2012), while SpiC (encoded by *Spic*) acts primarily as a repressor of transcription and is thought to counteract the action of SpiB and PU.1 (Schweitzer *et al.* 2006, Laramee *et al*. 2020), but all three are necessary for the proper function and development of both myeloid and lymphoid cells. PU.1 and SpiB are structurally and functionally similar – both bind the ETS binding sequence GGAA (Solomon *et al.* 2015).

Deletion of PU.1 results in murine embryonic lethality, with no development of B or T cells (Scott *et al.* 1994), whereas deletion of SpiB results in the development of B cells with a lack of responsiveness to BCR stimulation (Garrett-Sinha *et al.* 1999). Our lab has previously shown that deletion of both PU.1 (conditional in B cells) and SpiB (germline) in mice results in a total block in B cell development at the pre-B cell stage between the large pre-B and small pre-B steps and thus complete lack of mature B cells in tissue circulation (Batista *et al.* 2017). These cells are arrested in development at a stage of heightened proliferation signaling. This ultimately leads to the development of B cell acute lymphoblastic leukemia (B-ALL) at an incidence of 100% by 18 weeks of age (Batista *et al.* 2018). In human B-ALL patients, this translates as repression or loss-of-function mutations found in SpiB and PU.1 (Zhang *et al.* 2011). Other mouse models have been used in the past to generate leukemic mice with unique features, including

ETV6-RUNX1 fusion, E2A-PBX1 fusion, and the BCR-ABL fusion, among others (Jacoby *et al.* 2014).

1.4 B cell acute lymphoblastic leukemia

Interruptions in the highly regulated process of B cell development, such as deletion of PU.1 and SpiB can result in a B cell neoplasm, or leukemias. Leukemias are a category of cancer that localize to the blood and bone marrow. For the purpose of this thesis, the focus is on B cell acute lymphoblastic leukemia. Acute lymphoblastic leukemia (ALL) is the most prevalent type of cancer in young children, and despite the existence of many treatments, is still a leading cause of childhood cancer-related death (Iacobucci and Mullighan 2017). Of these cancers, approximately 80% of the ALL diagnoses in children are of the B cell lineage, called B-ALL (Iacobucci and Mullighan 2017). Pre-B cell acute lymphoblastic leukemia, or pre-B-ALL is a subset of B-ALL that involves mutations in transcription factors necessary for the development and functionality of the BCR (Roberts and Mullighan 2015). Pre-B-ALL tumors rely on increased signalling within the Janus kinase signal transducer and activator of transcription (JAK-STAT) signaling pathways that are typically controlled by interleukin-7 (IL-7) levels (Roberts *et al.* 2017). Activation of the JAK-STAT pathway ultimately results in the expression of genes involved in immune cell proliferation, stimulation, and survival (Roberts *et al.* 2017).

Cancer arises through an evolutionary selection process in which randomly generated mutations are selected for on the basis of their ability to increase cell proliferation, cell survival, inflammation, or any of the other hallmarks of cancer (Hanahan 2022). Cancer clones evolve into progressively more aggressive malignancies through the accumulation of beneficial so-called ‘driver’ mutations, and loss-of-function mutations (Greaves and Maley 2012, Swaminathan *et al.* 2015, DeKoter and Gibson 2016). It is thought that an average individual driver mutation gives a clonal advantage of approximately 0.4% but that the accumulation of such mutations, as well as epigenetic changes determine the overall clonal evolution. In human B-ALL, patients typically have a germline pioneer mutation in an oncogene, such as the ETV6-RUNX1 fusion. However, twin studies show that this pioneer oncogene fusion is not sufficient to cause B-ALL, as the twin with no additional somatic leukemogenic mutations did not develop leukemia, whereas the twin

that did have other mutations did develop B-ALL. This plus, the delay of 18 weeks in the PU.1/SpiB knockout mouse model suggests that the presence of a single germline mutated oncogene is not sufficient to cause leukemia, but that the procurement of other somatic driver mutations cumulates in leukemogenesis. A subset of pre-B-ALL, called Ph-like ALL, is characterized by mutations in B-cell transcription factors including Ikzf1 (Mullighan *et al.* 2008), Ikzf2, and Ikzf3 (Holmfeldt *et al.* 2013), and various mutations activating the JAK-STAT signaling cascade, such as activating mutations in JAK1 and JAK3, and mutations that impair negative regulators (Roberts and Mullighan 2015).

1.5 Mechanisms of mutagenesis and repair

Mutagenesis is an essential mechanism for genetic evolution but also plays a large part in aging and disease, especially in the generation of cancer. DNA can be damaged by exogenous chemicals or endogenous dysregulation resulting in mutations, and DNA polymerase occasionally makes mistakes during routine replication. However, cells have a multitude of checkpoint and repair mechanisms that act to mitigate the ramifications of this consistent DNA damage.

Endogenous sources of mutagenesis include replication errors, deamination, oxidation by ROS, and methylation. Unrepaired nucleotide base substitutions, insertions and deletions during DNA replication occur approximately once per million to hundred million cells each generation (Kunkel 2004), not including errors due to polymerase slippage, insertions of uracil into DNA, and mistakes in repair after topoisomerase nicking (Viguera *et al.* 2001, Andersen *et al.* 2004). Substitution mutations are classified into two types: transition mutations consist of a change from one purine to another or one pyrimidine to another, and transversion mutations involve changing a purine to a pyrimidine or vice versa. Deamination of bases can occur spontaneously or through the deaminase enzymes activation-induced cytidine deaminase (AID) and Apolipoprotein B mRNA editing enzyme catalytic polypeptide 1 (APOBEC1) during somatic hypermutation (Blanc and Davison 2010). Reactive oxygen species (ROS) in excessive amounts can cause a wide variety of DNA lesions and alterations resulting in mutations, estimated at nearly 100 different types of modifications depending on the specific ROS and nucleotide base involved. Additionally, ROS can attack the sugar-phosphate

backbone of DNA resulting in single-stranded breaks that may or may not be properly repaired (Giloni *et al.* 1981).

Exogenous sources of mutagenesis are wide and varied, including infrared and ultraviolet radiation, crosslinking agents, pollutants including polycyclic aromatic hydrocarbons, and other toxins. Radiation can cause damage through a variety of mechanisms, including production of ROS radicals, induction of single stranded breaks, and pyrimidine dimerization (Desouky *et al.* 2015, Henner *et al.* 1982, Chan *et al.* 1985). Other exogenous toxins and pollutants cause DNA breaks and mutations in an innumerable array of mechanisms.

Because of the wide variety of DNA lesions that can and do occur frequently, there are many repair mechanisms that occur naturally within cells, the most common of which are base excision repair (BER), nucleotide excision repair (NER), mismatch repair (MMR) and single stranded and double stranded break repair (SSBR and DSBR). BER is primarily used to correct damage to a single nucleotide base that does not cause major disruptions in the structure of the DNA alpha helix; this is recognized by one of many DNA glycosylase enzymes which initiates removal and replacement of the single affected nucleotide (Odell *et al.* 2013, Jacobs and Schar 2012). In contrast, NER is used to resolve lesions that cause changes in backbone structure but occurs in a similar fashion to BER, in which the lesion is excised and replaced with the signaling of many enzyme components but also involves chromatin remodelling (Scharer 2013). MMR is used to repair simple base mismatches and is led by the MutS homolog (MSH) group of peptides (Kunkel 2009).

1.6 The role of reactive oxygen species in leukemogenesis

Reactive oxygen species (ROS) describes a collection of molecules that originate from O_2 but undergo redox reactions or gain of electrons to become much more chemically reactive, hence the name. The term ROS includes hydrogen peroxide (H_2O_2), ozone (O_3), superoxide ($O_2^{-\cdot}$), and hydroxyl radical ($^{\cdot}OH$), among others. Cellular ROS are naturally generated due to oxidative phosphorylation in the mitochondria and can also appear

through exogenous sources. ROS are known to be necessary signaling molecules in a variety of cellular processes, but high levels of ROS lead to oxidative stress which can produce nucleic acid, protein, and lipid damage (Ray *et al*. 2012). Pre-B-cell expansion is marked by wide-ranging changes in metabolism, including increased levels of ROS that are involved in second messenger signaling (Ray *et al.* 2012). Typical ROS damage includes C>A transversion mutations due to oxidation of guanine residues, resulting in 8-oxoguanine mispairing with adenine (Kino *et al.* 2017). High ROS levels have been shown to stimulate survival as well as proliferation of leukemia cells (Prieto-Bermejo *et al.* 2018), and PU.1/SpiB knockout cell lines have shown a dependence on ROS to proliferate (Lim *et al.* 2020). Pro-B and pre-B cell lines from PU.1/SpiB knockout mice have increased levels of ROS compared to wildtype B-cells and have higher levels of 8-oxoguanine in their nuclei, indicating ongoing ROS damage within these cells (Lim *et al.* 2020).

1.7 The use of N-acetylcysteine as a therapeutic

N-acetylcysteine (NAC) is derived from the amino acid L-cysteine (**Figure 3**). It is currently approved by the FDA and Health Canada for a wide variety of uses, the most common being to treat acetaminophen overdose. NAC is also used as a long-term treatment for cystic fibrosis, to decrease inflammation and break down mucous (Conrad *et al.* 2014). NAC functions as an antioxidant through three related mechanisms: scavenging ROS through its free thiol group, reducing disulfide bonds, and acting as a precursor of glutathione, an essential repair molecule. Because of the extent to which ROS overactivity has been implicated in driving cancer, NAC is a very commonly studied potential therapeutic in cancer. NAC has been shown to reduce signaling in cancer cells for cell survival and cancer metastasis through reduction of ROS *in vitro* (Kwon 2021). Additionally, direct injection of NAC into an *in vivo* breast cancer model was able to significantly increase apoptosis from the center of the solid tumour (Agarwal *et al.* 2004), however it is not yet clear whether NAC has any ability to prevent cancer in any capacity.

In our lab, NAC has been shown to have opposing effects on ROS- and ROS-repair-related gene expression to H_2O_2, a common ROS (Lim *et al.* 2020). The addition of NAC

was also able to decrease proliferation of a primary leukemic cell line in a dose-dependent fashion (Lim *et al.* 2020), indicating potential sequestering of ROS proliferation signaling.

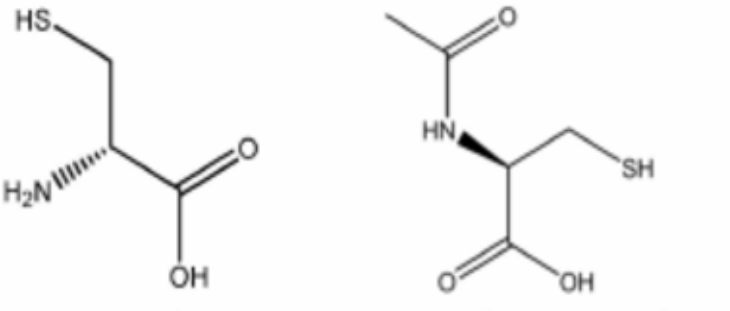

Figure 3. Chemical structures of N-acetylcysteine (right) and its amino acid derivative, L-cysteine (left).

1.8 Two mechanisms of mutation accumulation in Mb1-CreΔPB mice

Our lab has previously described a mouse model of B-ALL in which PU.1 and SpiB are effectively deleted in B cells under the control of the B cell-specific *Mb1* gene, termed Mb1-CreΔPB. Whole exome sequencing of Mb1-CreΔPB tumours to identify mutational signatures revealed two potential mechanisms of mutations occurring at different timepoints in tumour formation (Lim *et al.* 2020). A high variant allele frequency indicates that a mutation was obtained early on in clonal evolution and thus is carried by a large proportion of tumour cells. In contrast, a low variant allele frequency indicates a mutation gained late in clonal evolution, therefore being found in a lower proportion of cells. Lim *et al.* (2020) found that mutations with a high variant allele frequency were dominated by C>T transition mutations whereas low variant allele frequency mutations were more commonly C>A transversion mutations. This suggests that there are two distinct mechanisms for mutation acquisition that occur at different points in clonal evolution. C>T transition mutations are characteristic of action by APOBEC enzymes, specifically activation-induced cytidine deaminase (AID) (Casellas *et al.* 2016). On the other hand, C>A transversion mutations are typical of ROS damage, as described above. This begs questions as to the function of the two mutation classes and why or how these distinct processes are temporally controlled in tumours.

Within the sequenced Mb1-CreΔPB tumours, recurrent C>T mutations consistent with AID induction were observed in *Jak3* and *Jak1* (Lim *et al.* 2020). These mutations were predicted to be gain-of-function mutations, putatively resulting in increased levels of ROS due to increased JAK-STAT signaling. Treatment of Mb1-CreΔPB with ruxolitinib, a JAK inhibitor, was shown to significantly increase lifespan of these mice, and decrease the frequency of *Jak1* and *Jak3* mutations, indicating targeting of JAK mutant clones by ruxolitinib (Lim *et al.* 2020). Antioxidant genes were also shown to be downregulated in treated mice compared to control mice, suggesting a reduction in ROS levels in treatment mice (Lim *et al.* 2020). The focus of this thesis is to investigate whether heightened levels of ROS in Mb1-CreΔPB mice drive leukemogenesis through mutagenesis.

1.9 Research rationale and central hypothesis

Research from our lab has shown that mice lacking PU.1 and SpiB (Mb1-CreΔPB) develop leukemia with a median time to euthanasia of 18 weeks, and that at this endpoint, a subset of mutations is characterized by occurring later in clonal evolution with the mutations occurring according to the signature C>A transversions caused by ROS damage. Additionally, cell lines derived from our leukemic mouse model have been shown to have reduced growth and proliferation in the presence of the antioxidant NAC in a dose-dependent fashion.

We hypothesize that endogenous reactive oxygen species create mutations late in clonal evolution that act to drive growth of leukemic clones, and that this can be prevented by administration of the antioxidant NAC

To test this hypothesis, we proposed the following objectives:

1. Determine if administration of NAC at low doses delays onset of tumour growth and/or increases life span of the leukemic mouse model.
2. Determine if NAC reduces the accumulation of mutations in tumour clones, especially C->A transversion mutations.
    a. Identify recurrent mutations that potentially act as driver mutations of B-ALL progression
3. Evaluate changes in gene expression due to administration of NAC as it relates to tumour progression, ROS and metabolism regulation, and immune cell function to determine which cellular pathways are ultimately affected by the treatment.

Chapter 2

2 Materials and Methods

2.1 Breeding of mice

Mb1-CreΔPB mice were generated by crossing C57Bl/6 Mb1-Cre mice with C57Bl/6 *Spi1*$^{lox/lox}$*Spib*$^{-/-}$ mice (Batista *et al.* 2017). The colony was maintained by crossing *Mb1*$^{+/+}$*Spi1*$^{lox/lox}$*Spib*$^{-/-}$ female mice with *Mb1*$^{+/Cre}$*Spi1*$^{lox/lox}$*Spib*$^{-/-}$ male mice. *Mb1*$^{+/+}$*Spi1*$^{lox/lox}$*Spib*$^{-/-}$ mice were used as experimental controls (ΔB). The mice were housed in the West Valley Barrier under a 12-hour light/dark cycle and were fed irradiated chow and water *ad libidum*. Upon first signs of illness, the mice were euthanized using carbon dioxide in full accordance with the Western University Council on Animal Care.

2.2 Mouse genotyping

At 14-18 days of age, mice were ear tagged and had either tail tip or ear samples taken for genotyping using PCR and gel electrophoresis.

2.3 Water preparation

NAC-containing water was prepared using tap water and granulated N-acetyl-L-cysteine (>99%, Sigma Aldrich) and was filtered using 0.2 um PES filter units (VWR). Control water was prepared by filtering tap water. The prepared water was stored for a maximum of 2 months before use.

2.4 Water administration schedule

Mice were weaned from their mothers at day 21 of age, caged with 1-2 same-sex litter mates, and were randomly assigned to be administered either reverse-osmosis tap water or filtered tap water containing NAC. Water was administered through drinking bottles and was replaced for fresh water every 2-7 days. Water intake was monitored via water bottle weight every 2-3 days.

Table 1. Primer pair used for amplification of the *Cre* gene in Mb1-CreΔPB mouse genotyping samples.

Primer name		**DNA sequence (5’ -> 3’)**
Cre recombinase	F	AGATGCCAGGACATCAGGAACCTG
	R	ATCAGCCACACCAGACACAGAGATC

Mice on the 1g/L NAC study were administered 1g/L NAC-containing water starting at day 21 and ending at first sign of illness, according to **Figure 4A.** Mice on the 11-week endpoint study were administered 1g/L NAC water starting at day 21 and ending at 11 weeks of age, according to **Figure 4B.** Mice on the 6.5g/L NAC water study were administered 1g/L NAC-containing water starting at day 21, then male mice began receiving the increased dose at day 35 and female mice at day 42, according to **Figure 4C and D.**

2.5 Tissue extraction and flow cytometry

Thymus extracted from euthanized mice were homogenized and suspended in MACS buffer (500 mL 1x D-PBS, 1% 0.5M EDTA pH 8.0, 2.5g BSA fraction V). 1 million cells from the resulting single-cell suspension were stained with PE-conjugated CD19 antibody (BioLegend), a B cell marker, in preparation for flow cytometry. Flow cytometry results were analyzed using FlowJo (FlowJo LLC Ashland, OR).

2.6 RNA sequencing

RNA was isolated from the thymus of euthanized mice with the RNeasy Mini Kit (Qiagen, Hilden, Germany). RNA samples were sequenced using Truseq Stranded Total RNA Library Prep Kit and Illumina HiSeq4000 PE100 (Illumina, San Diego, CA) by the Genome Quebec Innovation Centre. The BAM files were trimmed using Trimmomatic and tested for differential expression using Salmonquant and DESeq2. These packages were all used courtesy of usegalaxy.org according to the workflow in **Figure 5.**

2.7 Pathway analysis

Heat maps and enrichment plots were generated using Gene Set Enrichment Analysis (GSEA) software using gene sets derived from the Panther database, or manually through literature search. Pathways were identified as potential targets of NAC using the Database for Annotation, Visualization and Integrated Discovery (DAVID) and Kyoto

Encyclopedia of Genes and Genomes (KEGG) pathways, and pathway diagrams were generated using DAVID.

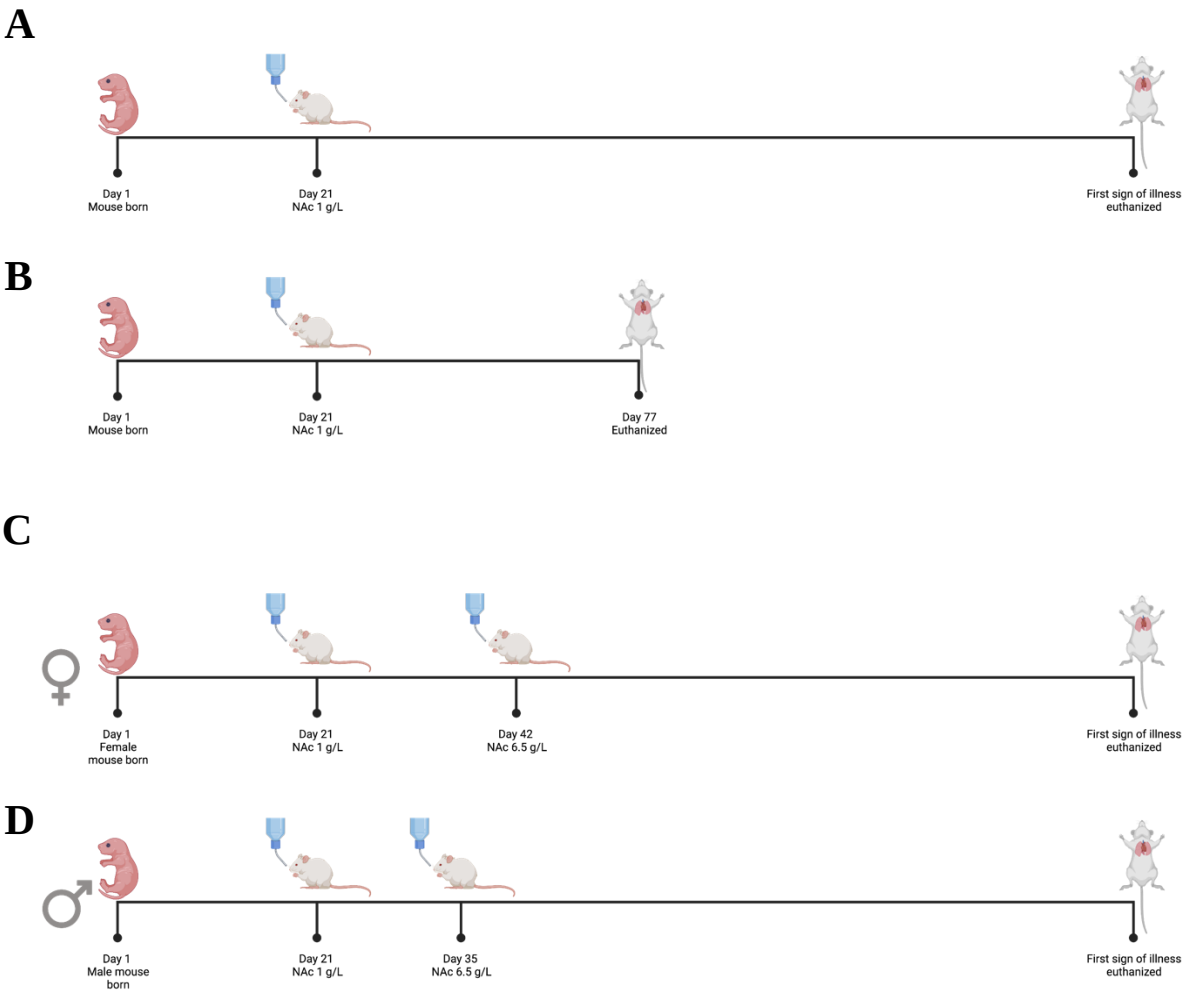

Figure 4. Treatment schedules for mice on NAC water studies.

A) Mice on the 1g/L study received 1g/L NAC water starting at day 21 and ending at first sign of illness. **B)** Mice on the 11-week study received 1g/L NAC water starting at day 21 and ending at 77 days (11 weeks) of age. **C)** Female mice on the 6.5 g/L study received 1g/L NAC water starting at day 21 and 6.5g/L starting at day 42, ending at first sign of illness. **D)** Male mice on the 6.5 g/L study received 1g/L NAC water starting at day 21 and 6.5g/L starting at day 35, ending at first sign of illness.

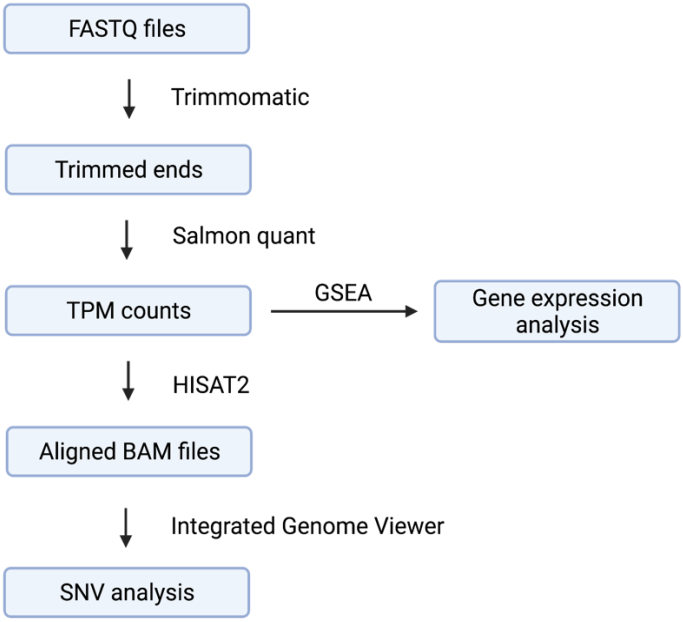

Figure 5. Workflow for the post-processing and analysis of RNA sequencing data.

FASTQ files were received from GenomeQuebec, and read ends were trimmed using Trimmomatic. Transcripts per million (TPM) raw gene expression counts were generated using SalmonQuant. These were analyzed using GSEA for gene expression analysis and generation of expression heatmaps. TPM counts were also aligned to the reference genome using HISAT2 to generate BAM files that were manually sorted through for single nucleotide variant (SNV) identification on Integrated Genome Viewer (IGV).

2.8 Statistical analysis

All data is reported as mean ±SEM. All statistical analyses were completed using Prism 8.0 (Graphpad Software, La Jolla, CA) with Student's t-test, Mann-Whitney test, ANOVA, or Log-rank (Mantel-Cox) tests. Mann-Whitney tests were performed in cases when standard deviations were considered significantly different between groups. Data was considered statistically significant with p values ≤ 0.05. $p \leq 0.05$ (*), $p \leq 0.01$ (**), $p \leq 0.001$ (***), $p \leq 0.0001$ (****).

Gene set enrichment analysis was analyzed using the Normalized Enrichment Score (NES) based on gene set size and overall correlation in expression. The False Discovery Rate (FDR) q-value gives the probability that the overall finding represents a false positive. Lower FDR q-values represent more certain results. Typically, gene sets are considered significantly enriched if the FDR q-value is below 0.05.

Chapter 3

3 Results

3.1 Administration of 1g/L N-Acetylcysteine in water did not confer a survival advantage to Mb1-CreΔPB mice compared to control water

We previously showed that NAC was able to reduce growth of a cultured leukemic cell clone in a dose-dependent fashion (Lim *et al.* 2020). Therefore, we hypothesized that Mb1-CreΔPB mice fed water supplemented with 1g/L of NAC would develop B-ALL and display signs of illness later than Mb1-CreΔPB mice fed control water. For this first experiment a low dose of 1g/L was used in order to alleviate potential toxicity to the animals. A total of 30 mice were included in this experiment: 15 mice on control water and 15 on N-acetylcysteine water **(Table 2)**. All cages of mice consumed an average of roughly 5 mL of water per day per mouse housed in the cage, irrespective of treatment group. The mice on control water and the mice on N-acetylcysteine water both developed leukemia and were euthanized upon first signs of illness including rapid, laboured breathing and hunched appearance, at a median age of 16.14 weeks **(Figure 6)**. When the mice were separated by sex, female mice displayed a larger difference in survival between treatment groups compared to male mice, although the difference did not reach statistical significance. Female mice on N-acetylcysteine had a median time to euthanasia of 15.86 weeks compared to 14.71 weeks for those on water with an overall median time to euthanasia of 15.07 weeks **(Figure 7A)**. Conversely, male mice on N-acetylcysteine had a median time to euthanasia of 17.43 weeks compared to 18.22 weeks for those on water with an overall median time to euthanasia of 18.22 weeks **(Figure 7B)**. This result suggests a biological difference between sexes causing a difference in the way mice respond to 1g/L NAC.

Of the 30 mice in this experiment, a subset had their thymuses removed for measurements of thymus weight (control n = 9, NAC n = 3), thymus cell count (control n = 8, NAC n = 6), and thymus CD19 positivity (control n = 7, NAC n = 5). There was no significant difference observed between treatment group in any of these categories

(Figure 8A, B, C). Frequency of CD19 positive cells within the thymus, a measure of B-cell frequency within a sample of cells, was consistently above 99% for both groups, with only one mouse falling between 97 and 98% **(Figure 8A)**. Three mice were not included in the statistical analysis for CD19 positivity (545, 552, and 597). 545 and 597 were not observed to be sick with leukemia, although displayed other signs of illness, requiring euthanasia according to suggestion by Animal Care Veterinary Services at Western University. Leukemic mice displayed typical symptoms such as a hunched appearance and rapid, laboured breathing, but ΔB mice (knockout for *SpiB* only) display the same symptoms when old or diseased other than B-ALL. The low thymus weight and lower than average CD19 positivity in these mice indicates that they were in the process of developing thymic B-ALL tumours but became sick due to other reasons before B-ALL could cause visible illness. For these reasons, mice 545 and 597 were also not included in thymus weight and cell count statistical analysis either. Conversely, mouse 552 was excluded due to improper laser calibration during flow cytometry, resulting in a large percentage of viable cells falling on the edges of the plot. Thymus weight and cell counts were still included for this mouse, as it displays the correct phenotype for B-ALL. A slight opposing trend was observed for thymus weight and thymus cell count in which control mice had lighter thymuses but a higher cell count **(Figure 8B, C)**.

Table 2. Characteristics of all mice on the 1g/L N-acetylcysteine water trial ordered by experimental group and date of birth.

All mice are of the Mb1-CreΔPB genotype. – indicates that data was not collected.

Mouse ID	Sex	Experi-mental Group	DOB	Treatm-ent Start	Age at death (weeks)	Thymus weight (g)	Thymus cell count (mill)	CD19 positivity (%)
680	f	NAC	28-01-21	18-02-21	16.29	-	-	-
685	f	NAC	28-01-21	18-02-21	14.00	-	80.5	99.7
696	m	NAC	28-02-21	21-03-21	14.14	-	58.0	99.2
697	m	NAC	28-02-21	21-03-21	18.71	-	-	-
511	f	NAC	29-03-21	19-04-21	14.14	0.6950	180.0	99.4
514	f	NAC	29-03-21	19-04-21	14.14	0.9230	152.0	99.6
851	m	NAC	20-04-21	12-05-21	20.14	-	-	-
856	m	NAC	20-04-21	19-04-21	20.14	-	-	-
537	f	NAC	11-05-21	02-06-21	16.29	-	-	-
545	f	NAC	12-05-21	02-06-21	22.29	0.0430	14.5	84.8
546	f	NAC	12-05-21	02-06-21	22.71	-	-	-
557	m	NAC	24-05-21	14-06-21	16.14	-	-	-
558	m	NAC	24-05-21	14-06-21	15.14	-	-	-
962	f	NAC	16-06-21	07-07-21	15.86	0.8350	222.0	99.5
963	f	NAC	16-06-21	07-07-21	14.14	-	-	-
690	f	Control	19-02-21	03-12-21	15.43	-	167.0	99.7
692	f	Control	19-02-21	03-12-21	10.57	-	34.6	99.6
512	m	Control	29-03-21	19-04-21	18.29	0.3553	-	-
513	m	Control	29-03-21	19-04-21	19.00	-	-	-
853	f	Control	20-04-21	19-04-21	14.00	0.9810	248.0	99.7
854	f	Control	20-04-21	19-04-21	15.86	-	-	-
858	f	Control	20-04-21	19-04-21	18.14	0.1558	-	-
552	m	Control	14-05-21	04-06-21	17.57	-	-	94.7
555	m	Control	14-05-21	04-06-21	20.00	0.6862	120.0	-
593	f	Control	07-06-21	28-06-21	11.29	0.7637	-	-
597	f	Control	07-06-21	28-06-21	7.29	0.0469	78.4	27.3
574	m	Control	14-06-21	07-07-21	18.14	0.4606	138.0	97.4
575	m	Control	14-06-21	07-07-21	16.14	0.3640	83.0	99.6
057	f	Control	01-08-21	23-08-21	14.71	0.4814	210.0	99.7
058	f	Control	01-08-21	23-08-21	17.43	0.6123	178.0	99.5

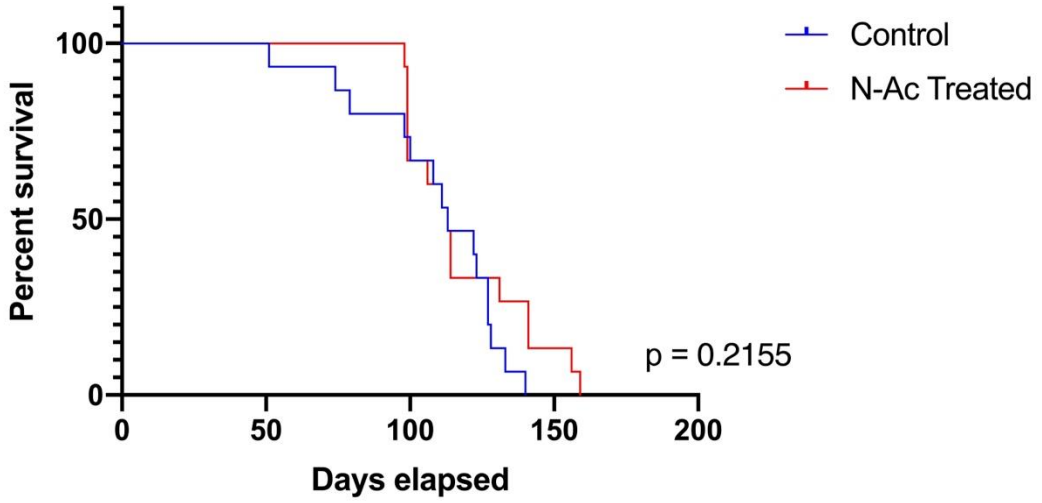

Figure 6. Mice administered 1g/L of N-acetylcysteine through drinking water did not display an increase in survival compared to mice fed control water.

Kaplan-Meier survival curves of Mb1-CreΔPB mice administered either 1g/L N-acetylcysteine in drinking water or regular reverse-osmosis tap water starting at day 21 of age. Mice on both treatment and control water had a median time to euthanasia of 16.14 weeks. Log-rank (Mantel-Cox) test, control n = 15, N-acetylcysteine n = 15, p = 0.2155.

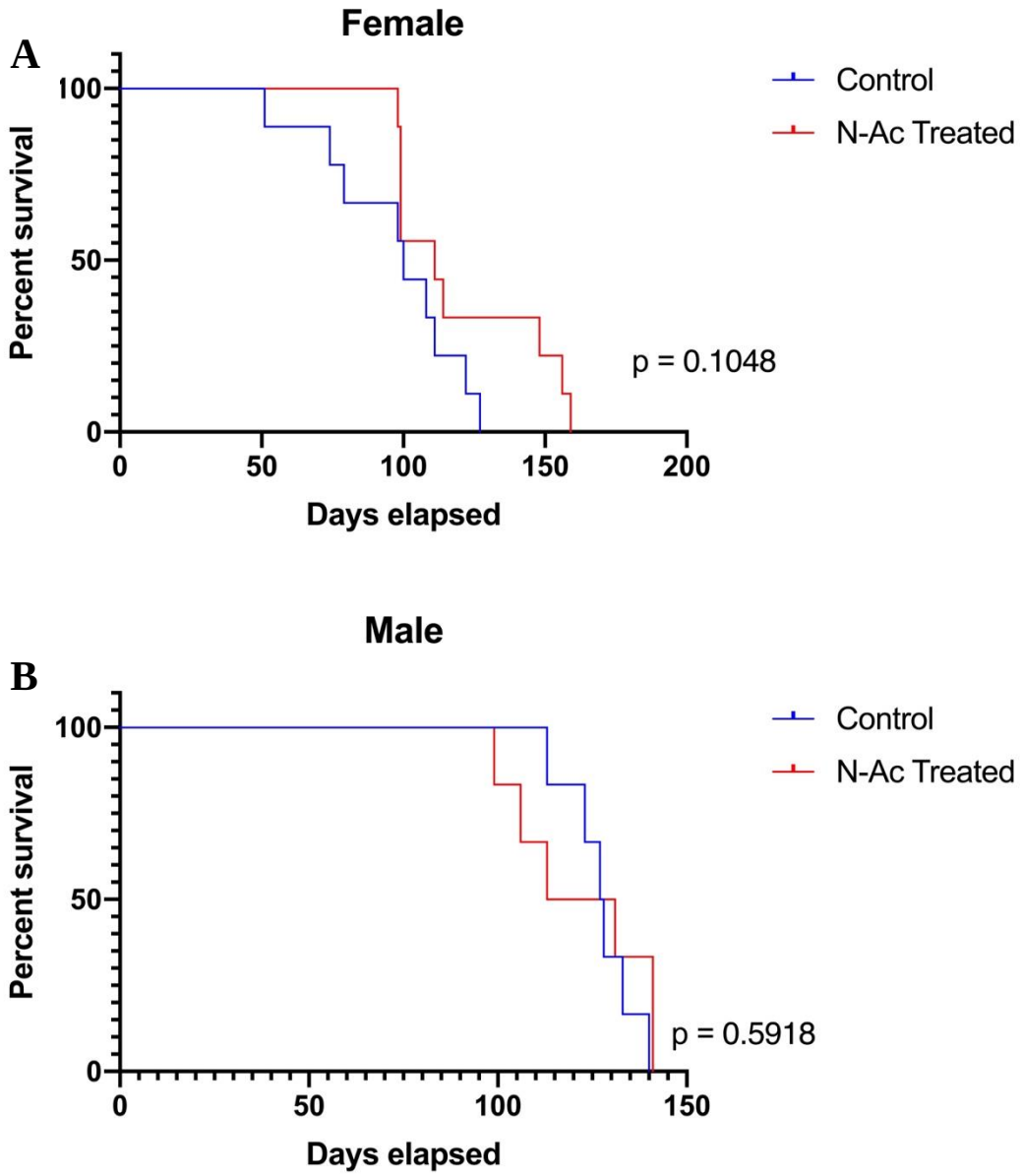
A
Female
Percent survival
100
50
0
0
50
100
150
200
Days elapsed
Control
N-Ac Treated
p = 0.1048
B
Male
Percent survival
100
50
0
0
50
100
150
Days elapsed
Control
N-Ac Treated
p = 0.5918

Figure 7. Mice administered 1g/L of N-acetylcysteine through drinking water displayed differences in survival between sexes, but no difference in survival compared to control mice.

Kaplan-Meier survival curves of the same Mb1-CreΔPB mice separated by sex. **A)** Female mice on N-acetylcysteine had a median time to euthanasia of 15.86 weeks compared to 14.71 weeks for those on water with an overall median time to euthanasia of 15.07 weeks. Log-rank (Mantel-Cox) test, control n = 9, N-acetylcysteine n = 9, p = 0.1048. **B)** Male mice on N-acetylcysteine had a median time to euthanasia of 17.43 weeks compared to 18.22 weeks for those on water with an overall median time to euthanasia of 18.22 weeks. Log-rank (Mantel-Cox) test, control n = 6, N-acetylcysteine n = 6, p = 0.5918. Between these two curves, although not significant, female mice displayed a larger difference between treatment and control groups compared to male mice.

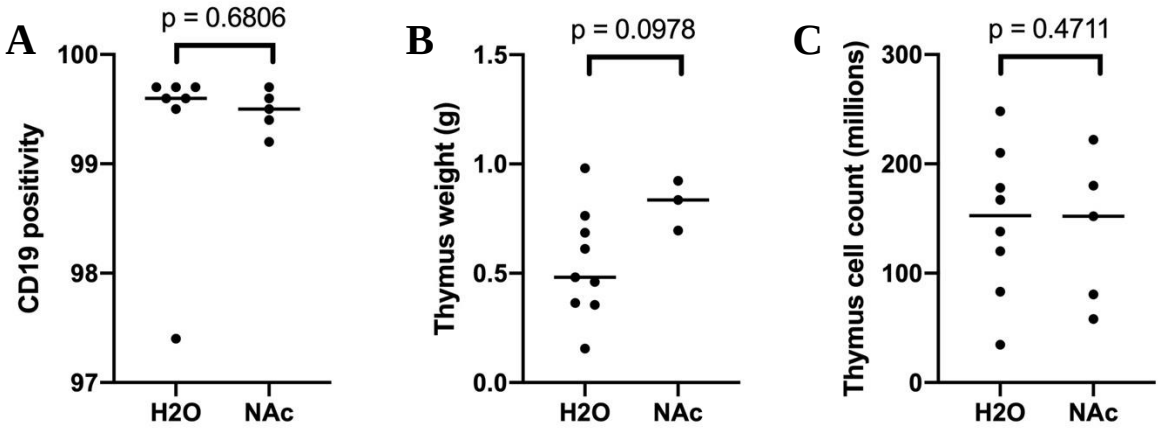

Figure 8. There is no significant difference in thymus CD19 positivity, thymus weight, or thymus cell count in sick mice between the N-acetylcysteine treatment and control groups.

CD19 positivity, thymus weight, and thymus cell count from Mb1-CreΔPB mice fed either control or 1g/L N-acetylcysteine water. **A)** CD19 positivity unpaired t test, control n = 7, N-acetylcysteine n = 5, p = 0.6806. **B)** Thymus weight unpaired t test, control n = 9, N-acetylcysteine n = 3, p = 0.0978. **C)** Thymus cell count unpaired t test, control n = 8, N-acetylcysteine n = 5, p = 0.8256.

3.2 Female mice weigh significantly less than male mice, and therefore receive a higher NAC dose per body weight

All experimental mice were weighed every 1-3 days to ensure sufficient water intake. While there was a significant difference in weight between treatment and control male mice, there were no visible health differences **(Figure 9A)**. However, when observing only the averaged weights at day 100 and beyond, there were significant differences between treatment and control groups in both males and females **(Figure 9B)**. By 100 days, there were fewer mice alive in almost every group, leaving 6 control male mice, and 5 mice in each of the other three treatment/sex combinations. Irrespective of treatment group, there was a significant difference observed in both daily weights of male and female mice and peak weight reached by each sex, with female mice consistently weighing less than male mice **(Figure 10A and B)**. Additionally, the amount of water ingested by males and females was not significantly different with an average daily consumption of 6.00 g for males and 5.619 g for females **(Figure 10C)**. This corresponds to female mice weighing less than 75% that of male mice and female mice ingesting over 90% that of male mice. This observation suggests a difference in NAC dose per body weight in male and female mice and prompted an investigation into correlations between body weight and effectiveness of NAC treatment.

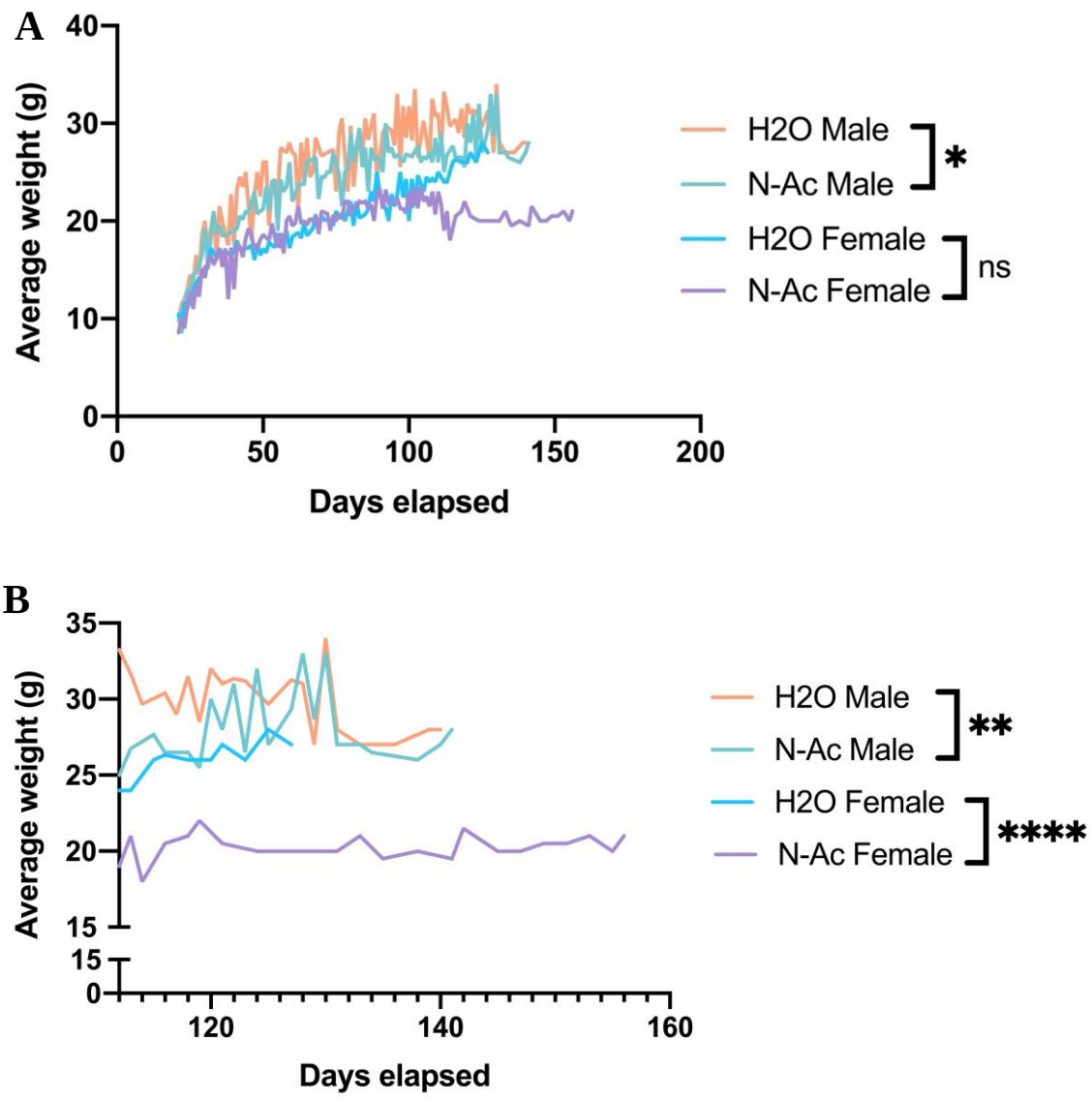

Figure 9. Averaged mouse weights split by treatment group and sex.

Mb1-CreΔPB mice on the water study were weighed every 1-3 days. While the weights between treatment and control groups for the male mice were statistically significant, there was no biologically relevant difference between treatment groups within sex, except for the female mice after day 100. At day 21, control male n = 6, NAC male n = 6, control female n = 9, NAC female n = 9. **B)** After day 100, control male n = 6, NAC male n = 5, control female n = 5, NAC female n = 5.

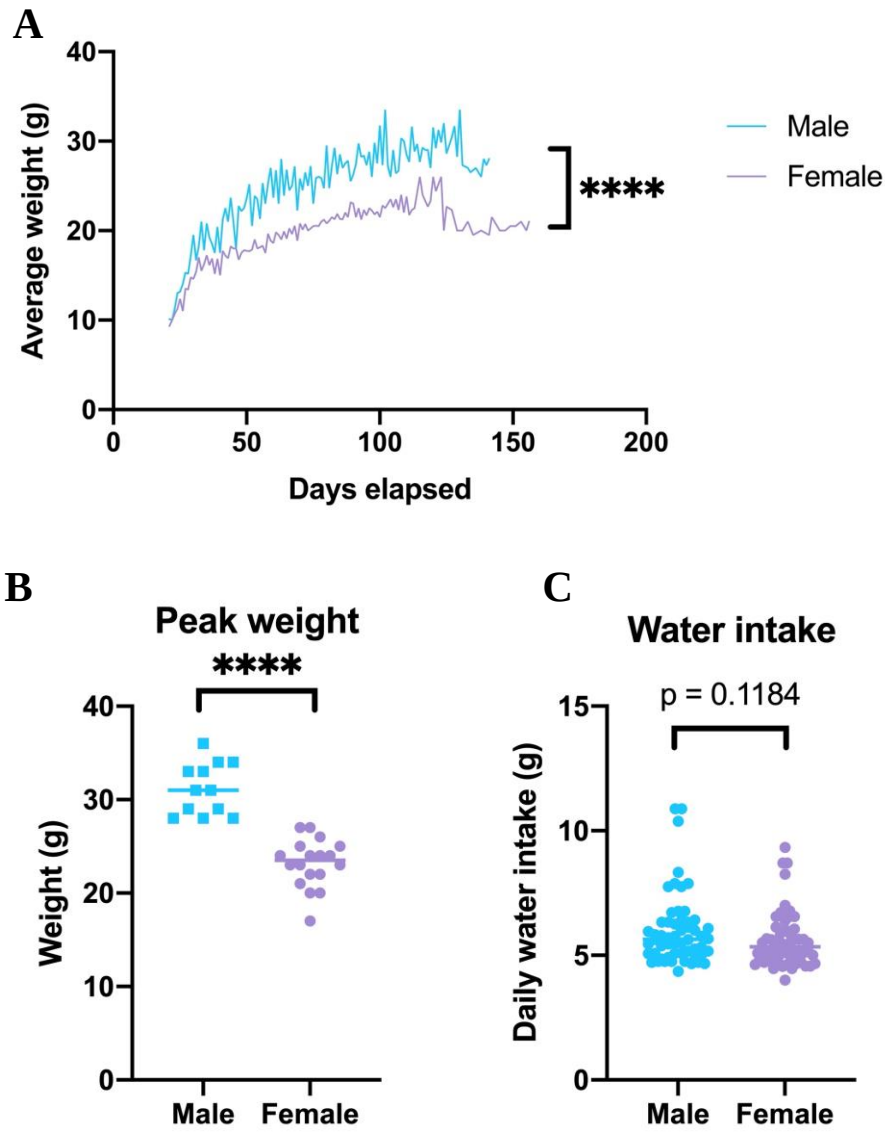

Figure 10. Adult female mice weigh on average significantly less than adult male mice

A) Male mice weigh significantly more throughout the course of the water study compared to female mice. Unpaired t test, male n = 12, female n = 18, $p < 0.0001$. **B)** The peak weight reached by male mice is significantly higher than the peak weight of female mice. Unpaired t test, male n = 12, female n = 18, $p < 0.0001$. **C)** The amount of water ingested by males is not significantly different from that ingested by females. Data points represent daily water intake averaged between 3 sets of cage mated mice between 21 and 77 days of age. Unpaired t test male n = 6, female n = 6, $p = 0.1184$.

3.3 Female mice that weighed less tended to survive longer when treated with 1g/L NAC

Based on the significant differences observed in female mice weight after day 100, we hypothesized that the mice that weigh less receive a higher dose per bodyweight and can therefore survive longer. When NAC-treated female mice were split into groups that survived less than or longer than 16 weeks (112 days), a significant difference was observed in their weights, with mice living longer than 16 weeks weighing significantly less over the course of their lives **(Figure 11A)**. Furthermore, when split into groups that survived less than 16 weeks, between 16 and 20 weeks, and longer than 20 weeks, this trend held up, with mice surviving the longest having the lowest body weight since weaning **(Figure 11B)**. Conversely, when control mice were split in the same fashion (surviving less than or longer than 16 weeks), the same trend was not observed **(Figure 11C)**. This result suggests that the differential survival was due to a combination of body weight and NAC dosage, and not just body weight alone.

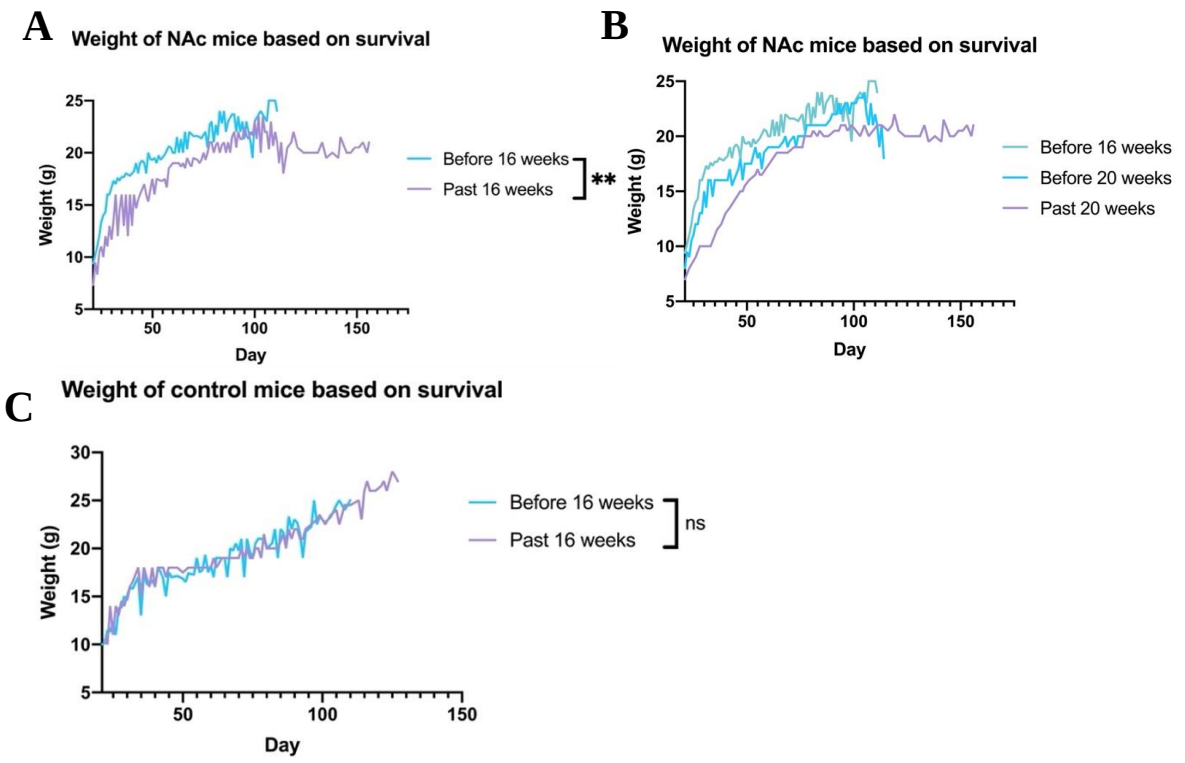

Figure 11. Female mice on NAC that weigh less survive longer, whereas female control mice have no difference in weight based on survival.

The overall median time to euthanasia for all mice on the 1 g/L study was approximately 16 weeks. **A)** When observing female mice, those treated with NAC differ significantly in their average weights through the course of their lifespans when comparing those who survived more than the median 16 weeks and those who survived less than the median 16 weeks (unpaired t test p=0.0098). **B)** A comparison of female mice that survived less than 16 weeks, between 16 and 20 weeks, and more than 20 weeks. **C)** Female control mice tended to weigh the same amount regardless of how long they survived (unpaired t test p=0.0511).

3.4 Mice within the same litter tend to develop leukemia at a similar timepoint compared to non-littermates

Mice were placed in treatment or control groups with 2-3 littermates in each cage, in accordance with veterinary recommendations provided by Western's ACVS. There was a tendency observed for mice within the same litter to develop leukemia at a similar timepoint compared to mice from different litters but on the same treatment group. A one-way ANOVA and post-hoc Tukey test indicated a significant difference among means between litter groups all on N-acetylcysteine water **(Figure 12A)**. Of the 7 litter groups with two mice each, 4 had the two mice develop illness within 7 days of each other, and 5 within two weeks. One particular cage of mice housed three mice treated with N-acetylcysteine: two mice from one litter (mouse tag 545 and 546) and one mouse from a different litter (tag 537) but born on the same day. All three mice were housed together for the duration of the experiment. The two mice from the same litter developed illness within three days of each other, while the individual mouse from the separate litter developed illness 6 weeks before the earlier of the two litter-mates **(Figure 12B)**. These results suggest a genetic or inherited epigenetic influence on progression of leukemia in the Mb1-CreΔPB mouse model.

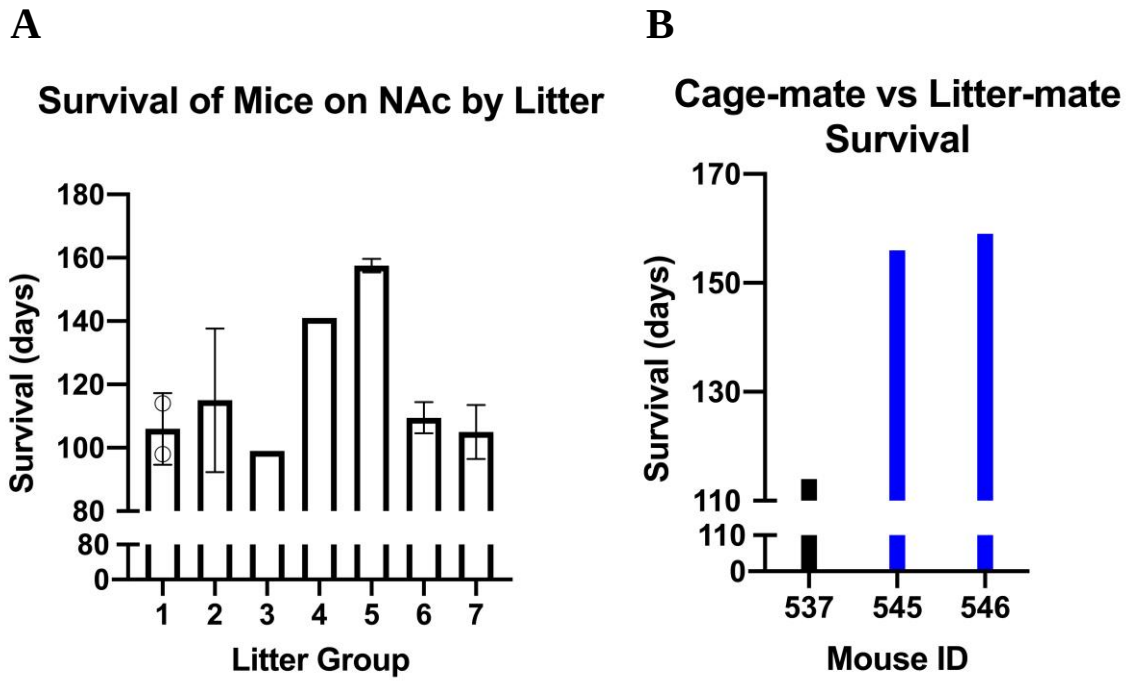

Figure 12. Mb1-CreΔPB mice from the same litter tend to develop leukemia at similar time points.

Mice from a total of 8 different litters were placed in the 1g/L N-acetylcysteine treatment group; 7 of these litters provided two mice of the same sex and one litter provided one female mouse. **A)** Of the 7 litter groups with two mice each, 4 had the two mice develop illness within 7 days of each other, and 5 within two weeks. A one-way ANOVA indicated a significant difference among means ($p = 0.0054$). **B)** One cage group was comprosed of two female mice from one litter (tag 545 and 546) and one female mouse from a separate litter but born on the same day (tag 537). The two mice from the same litter developed illness at days 156 and 159, much more similar than the third mouse, which developed illness at day 114.

3.5 Administration of 1g/L of N-acetylcysteine resulted in delayed tumour growth at 11 weeks of age

To determine if there were differences in the timeline of leukemic onset, and to potentially visualize tumours before full growth, an intermediate timepoint was selected to euthanize mice. Our lab previously showed that Mb1-CreΔPB mice begin to display infiltration of CD19-positive cells in the thymus at 11 weeks of age (Batista *et al.* 2018). Thus, to measure early leukemic progression, an 11-week endpoint was selected as a starting point to see if differences between treatment groups would be observed A total of 16 mice were included in this intermediate timepoint experiment **(Table 3)**. At 11 weeks, the mice fed 1g/L NAC water had significantly lower frequencies of CD19 positive leukemia cells within the thymus **(Figure 13A)**. With the exception of two pairs of litter mates (black and purple data points), the CD19 positivity of littermates fell within 10% of each other, and 5 of 8 pairs within 5% of each other. In the two litter groups for which CD19 positivity was not similar, one mouse in each pair had very low CD19 positivity levels (below 4%) while the other mouse had a moderate CD19 positivity (between 40 and 60%). Moderate levels of CD19 positivity (above 15 but below 80%) were not observed in any other mouse in any of the N-acetylcysteine water experiments. There was no significant difference observed between treatment groups in terms of thymus weight and thymus cell count, but the same opposing trend was observed as in the initial 1g/L experiments **(Figure 13B, C)**. Interestingly, the same control mice that presented with low CD19 positivity were the same three mice that had thymus cell counts within the higher range for that group **(Figure 13A, C, Table 3)**. In conclusion, 62.5% of control mice presented with evidence of a tumour, compared to 12.5% of treated mice, suggesting a tumour-suppressing ability of NAC at this timepoint.

Of the total 16 mice on this experiment, four female mice originated from the same litter (tags 235-238). The mice were randomly split into groups of two, one group receiving control water, and the other N-acetylcysteine water. At the 11-week timepoint, there were significant differences observed in all three measures of CD19 positivity, thymus weight, and thymus cell count **(Figure 14A, B, C)**. The trends of this select group of mice matched the trends observed in the overall experiment **(Figure 13 and 14)**. The mice

receiving N-acetylcysteine had significantly lower CD19 positivity (below 4%) than their littermates receiving control water (above 85%) **(Figure 14A)**. Additionally, the N-acetylcysteine treated mice had significantly lighter thymuses and significantly higher cell counts when compared to their control littermates **(Figure 14B, C)**.

Furthermore, visible differences in the thymus tissue of these four littermates were observed. The two control mice (tags 235 and 236) had a deeper red colour compared to the N-acetylcysteine-treated mice both in whole extracted tissue and homogenized cells **(Figure 15)**. However, NAC mice euthanized upon sickness had significantly higher expression of a vascularity cell marker CD31 (encoded by *Pecam1*) **(Figure 16)**. *Pecam1* expression was determined using RNA sequencing as described in sections 2.6 and 3.8. The differences in thymus weight and cell count mentioned above were not translated visually in terms of thymus size, with all four thymuses being relatively the same size as a typical mouse heart. Taken together, these results suggest that 1g/L of NAC suppresses the onset of leukemogenesis at 11 weeks of age.

Table 3. Characteristics of all mice on the 11-week N-acetylcysteine water trial.

All mice are of the Mb1-CreΔPB genotype. – indicates that data was not collected.

Mouse ID	Sex	Experi-mental Group	DOB	Treatm-ent Start	Date of euthan-asia	Thymus weight (g)	Thymus cell count (mill)	CD19 positivi-ty (%)
051	m	NAC	29-07-21	19-08-21	14-10-21	0.0301	23.6	5.81
053	m	NAC	29-07-21	19-08-21	14-10-21	0.0383	32.4	12.40
230	m	NAC	18-10-21	08-11-21	03-01-22	0.0542	32.0	58.80
232	m	NAC	18-10-21	08-11-21	03-01-22	0.0486	54.0	3.13
237	f	NAC	27-10-21	27-10-21	12-01-22	0.0762	113.6	2.49
238	f	NAC	27-10-21	27-10-21	12-01-22	0.0705	124.8	1.37
301	f	NAC	09-11-21	09-11-21	25-01-22	0.0895	119.2	0.68
303	f	NAC	09-11-21	09-11-21	25-01-22	0.0799	136.8	1.73
060	m	Control	01-08-21	22-08-21	19-10-21	0.0420	10.3	88.20
061	m	Control	01-08-21	22-08-21	19-10-21	0.0445	6.6	82.80
226	f	Control	06-10-21	06-10-21	22-12-21	0.0701	107.0	5.60
229	f	Control	06-10-21	06-10-21	22-12-21	0.0162	52.0	0.71
235	f	Control	27-10-21	27-10-21	12-01-22	0.1772	30.4	91.20
236	f	Control	27-10-21	27-10-21	12-01-22	0.1423	24.8	89.10
329	m	Control	25-11-21	16-12-21	10-02-22	0.0773	21.0	41.80
331	m	Control	25-11-21	16-12-21	10-02-22	0.0738	88.0	0.52

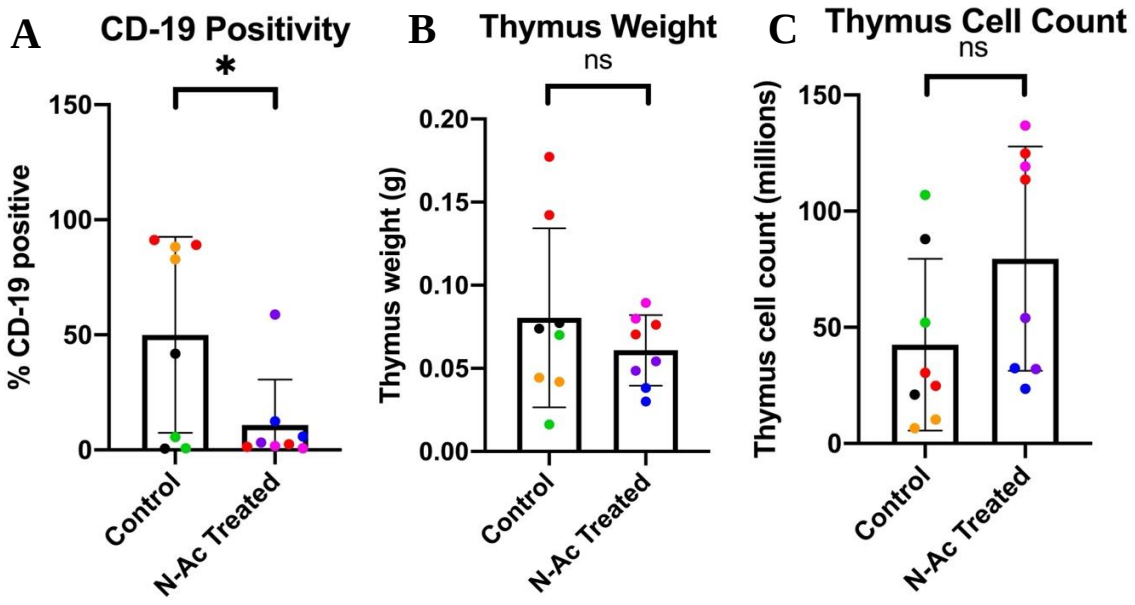

Figure 13. Mb1-CreΔPB mice treated with 1g/L NAC had significantly lower CD19 positivity, indicating lower B cell infiltration into their thymuses while thymus weight and cell counts were not significantly different.

Mice were administered 1g/L NAC or control water from day 21 of age and euthanized at day 77 when thymuses were extracted. **A)** Mice on NAC water displayed significantly lower CD19 positivity, marking lower B-cell infiltration to the thymus on average compared to control mice. Unpaired t test, control n = 8, NAC n = 8, p value = 0.0332. **B)** Thymus weight was observed to be similar between treatment and control gorups. Unpaired t test, control n = 8, NAC n = 8, p value = 0.5036. **C)** There was no significant difference observed between treatment and control groups in thymus cell counts. Unpaired t test, control n = 8, NAC n = 8, p value = 0.0551. Data points of the same colour represent individual mice from the same litter.

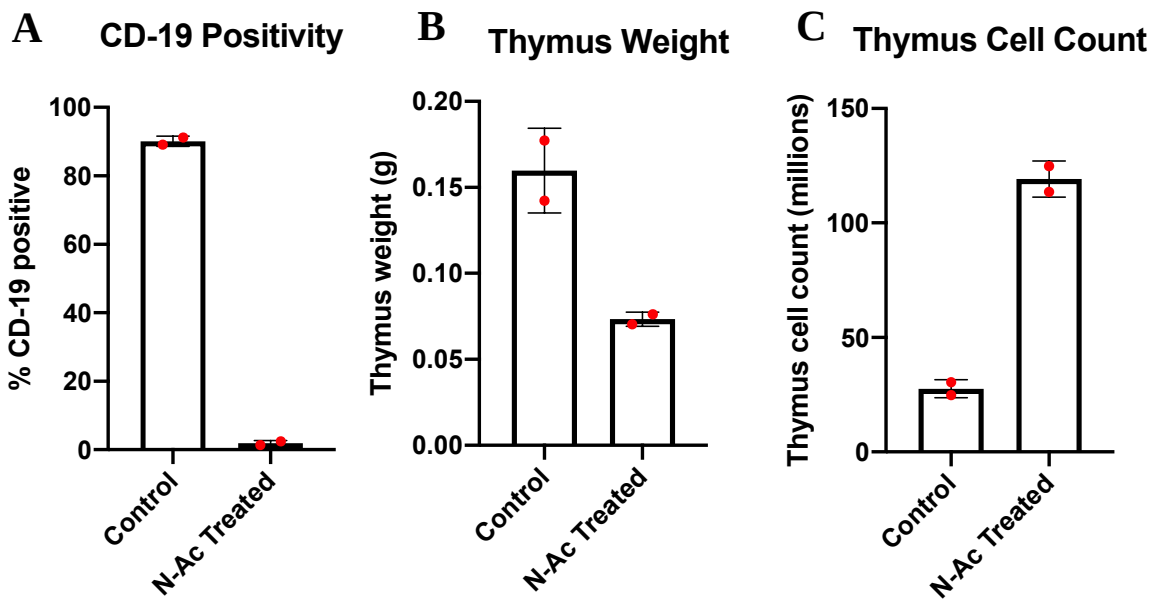

Figure 14. Four Mb1-CreΔPB mice from the same litter split into treatment and control water groups displayed significant differences in thymic CD19 positivity, weight, and cell count after 11 weeks.

Four female Mb1-CreΔPB mice from the same litter were split randomly into two cages that received either 1g/L NAC or control water. **A)** The mice on NAC-treated water had lower CD19 positivity compared to control mice. Unpaired t test, control n = 2, treatment n = 2, p value = 0.0002. **B)** NAC-treated mice had lower thymus weight compared to control mice. Unpaired t test, control n = 2, treatment n = 2, p value = 0.0394. **C)** NAC-treated mice had higher thymus cell counts compared to control mice. Unpaired t test, control n = 2, treatment n = 2, p value = 0.0046.

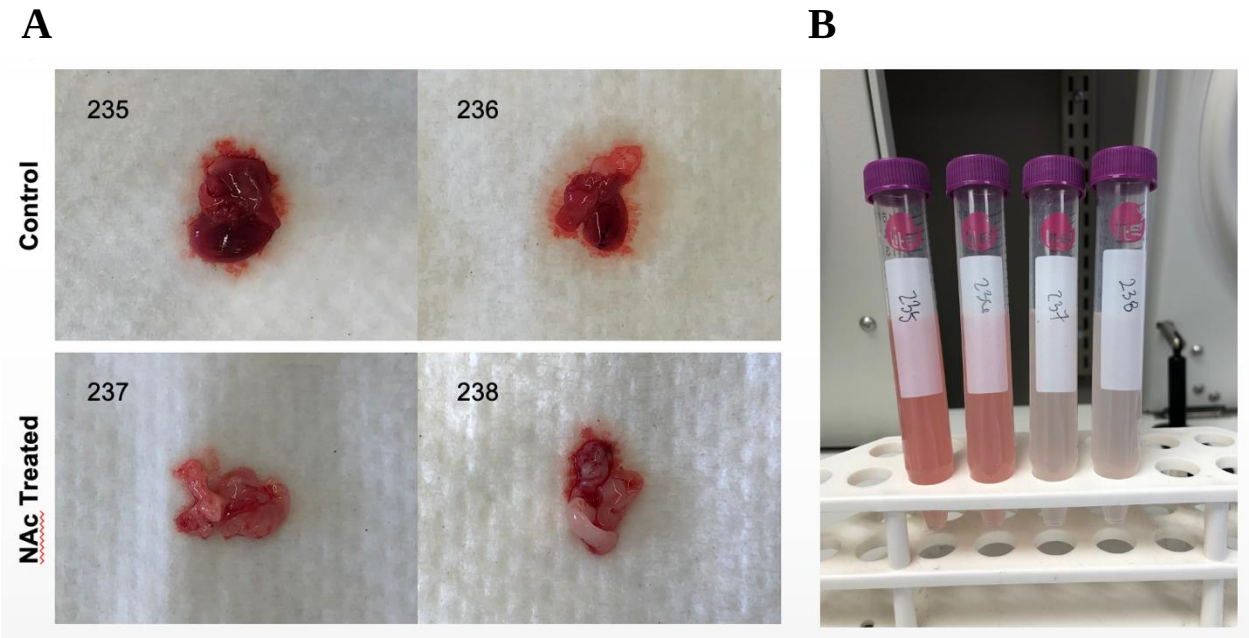

Figure 15. Thymuses extracted from control mice tended to be redder in colour compared to thymuses from mice receiving NAC at the 11-week timepoint.

All thymuses were approximately the same size as a healthy mouse heart, but control thymuses were redder in both their whole tissue form **(A)**, and in homogenized single cell suspensions **(B)**.

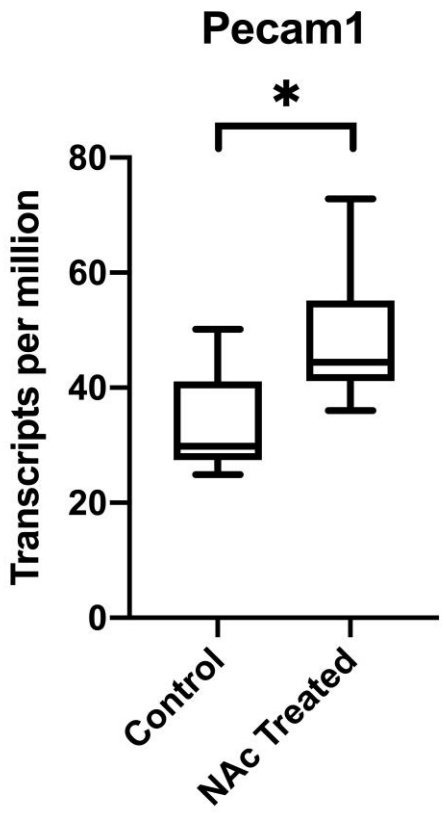

Figure 16. Mice treated with 1g/L NAC have significantly higher expression of vasculature marker gene *Pecam1*.

Raw TMP counts of *Pecam1* expression show significantly increased expression in NAC-treated mice compared to control mice. Mann-Whitney test p=0.0205.

3.6 Mice with low CD19 positivity have lower thymus cell count to thymus weight ratios

In the 11-week trial, it was noted that thymus CD19 positivity fell into one of three clear bins: low CD19 positivity (<15%), high CD19 positivity (>80%), or somewhere in the middle, with the majority falling into one of the two extreme bins. Thymuses with low CD19 positivity were observed to have significantly higher thymus cell count to weight ratios (indicating a light thymus with many cells) compared to thymuses with high CD19 positivity (**Figure 17A**). Thymuses with mid (between 15-80%) CD19 positivity had cell count to weight ratios between the two extremes, albeit with a mean much closer to that of the high CD19 positivity bin. When cell count to weight ratio was plotted against CD19 positivity, a linear regression indicated that the slope was significantly non-zero with a p-value of 0.0007 (**Figure 17B**). This indicates that there is a correlation between tumor progression, as measured by CD19 positivity, and thymus cell count to weight ratio, potentially due to differences between cell type and/or morphology between the groups.

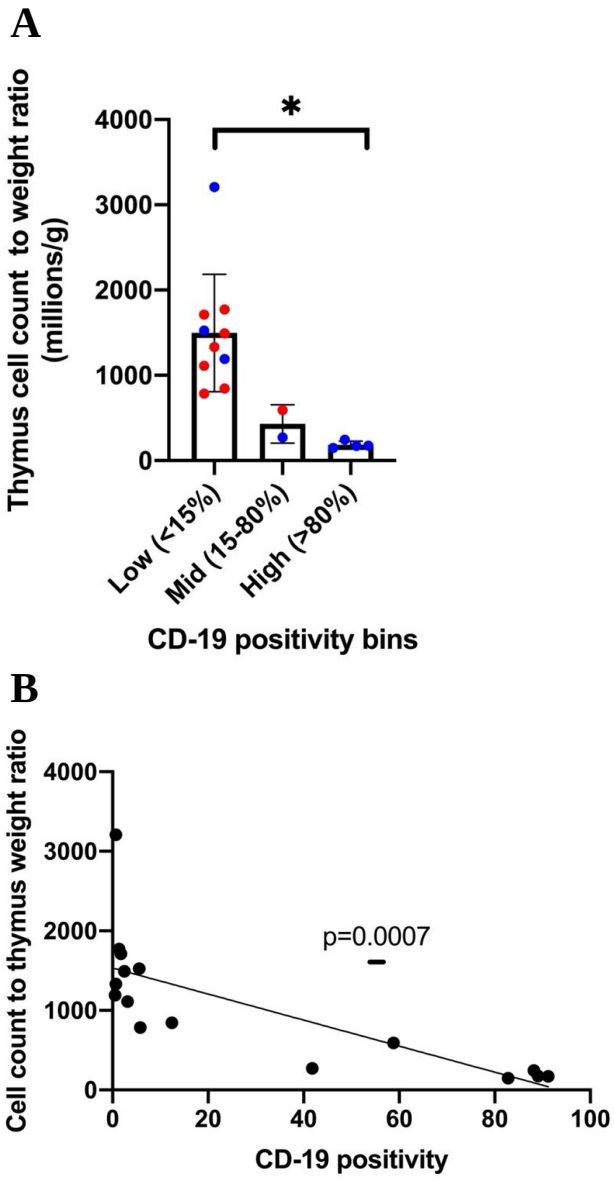

Figure 17. Mice with lower B cell infiltration into the thymus have lower thymus cell count to thymus weight ratios.

A) Mice were grouped into three bins of CD19 positivity: low (<15%), mid (15-80%), and high (>80%). The mice with low CD19 positivity had significantly higher thymus cell count to weight ratios compared to the mice with high CD19 positivity, whereas the mice with mid CD19 positivity fell between the two extreme groups. One-way ANOVA with Tukey's multiple comparison test indicated p values of: low vs mid p=0.0781, low vs high p=0.0053, mid vs high p=0.8756. **B)** A linear regression of these individual data points indicated a slope of non-zero with a p-value of 0.0007.

3.7 6.5g/L NAC water does not confer a survival advantage

Observed differences between male and female survival on 1g/L NAC, as well as significant differences in tumour progression at 11 weeks suggested that the 1g/L NAC dose was too low at adult body weight to cause differences in life span and suggested that a higher dose might be more effective in preventing B-ALL development. The oral mouse LD50 for NAC is >3g/kg (Gosselin *et al.* 1984), which for a 15 g mouse would correspond to 45 mg, or 45 mL of 1g/L NAC water or 6.9 mL of 6.5 g/L NAC water. A given mouse ingests on average between 5-6 g of water per day **(Figure 10C)**. To reduce the risk of reaching the LD50 NAC dose, it was determined that at a 15 g body weight, 6.5 g/L would not be unsafe, but that at lower weights, especially weights at weaning (between 7-10 g) 6.5g/L may exceed the LD50. To circumvent this, Mb1-CreΔPB mice were administered 1 g/L NAC water starting at day 21 after birth and then switched to the higher dose at a later defined timepoint. It was observed that all male mice reach 15 g in body weight at 5 weeks of age, whereas female mice reach 15 g by 6 weeks and thus these were the selected timepoints for dosage increase (**Figure 18**). Additionally, with a molar mass of 163.19 g/mol, 6.5 g/L is equivalent to 40mmol, which is a dose that has been shown to inhibit ROS in other studies (Laurent *et al.* 2008). This study is ongoing but at present there have been 15 Mb1-CreΔPB mice on NAC water and 13 Mb1-CreΔPB mice on control water (**Table 4**). In total 7 NAC mice and 3 control mice have been euthanized and there are no significant differences observed in lifespan at this heightened dose (**Figure 19**). Similarly to the 1g/L trial, there is no significant difference in CD19 positivity or thymus cell count between sick mice of each group, however, 6.5g/L NAC-treated mice have significantly lighter thymuses compared to control mice (**Figure 20**). Taken together, these results suggest that 6.5g/L NAC does not provide a survival advantage to Mb1-CreΔPB mice but there is a difference in how far the tumour progresses in terms of size before physical illness is reached.

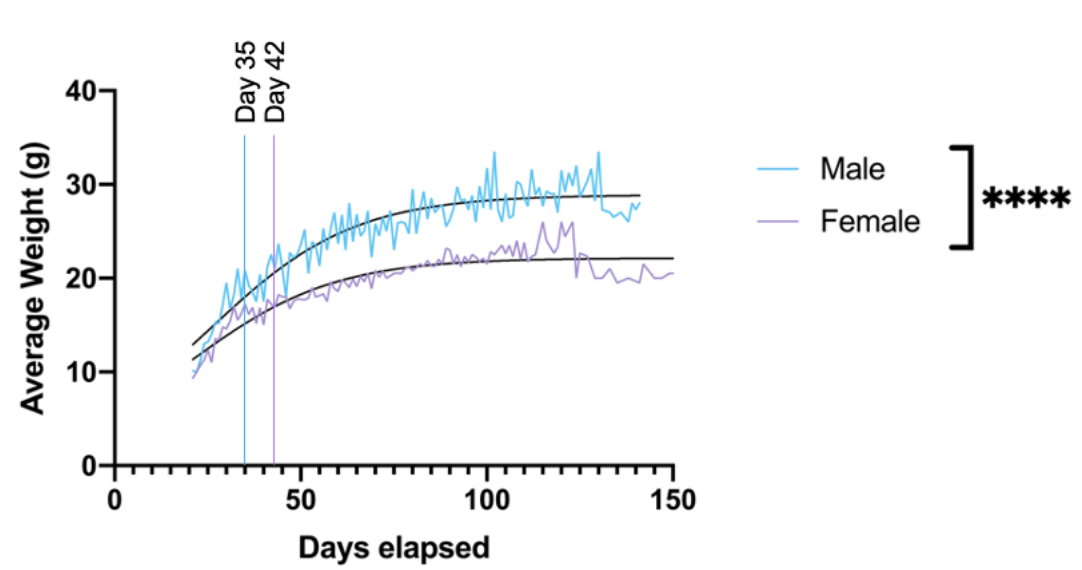

Figure 18. Male and female mouse weights averaged over time.

Male mice reach the selected threshold weight of 15g by week 5 (35 days of age) whereas female mice reach 15g by week 6 (42 days of age).

Table 4. Characteristics of all mice on the 6.5g/L N-acetylcysteine water trial.

All mice are of the Mb1-CreΔPB genotype. – indicates that data was not collected.

Mouse ID	Sex	Experi-mental Group	DOB	Treatm-ent Start	Date of euthan-asia	Thymus weight (g)	Thymus cell count (mill)	CD19 positivi-ty (%)
330	f	NAC	25-11-21	16-12-21				
333	f	NAC	25-11-21	16-12-21	28-03-22	0.7423	190.4	98.9
362	f	NAC	04-12-21	23-12-21	28-03-22	0.4214	207.2	99.8
363	f	NAC	04-12-21	23-12-21	07-04-22	0.2487	55.7	99.1
435	f	NAC	26-01-22	17-02-22	13-05-22	-	-	-
436	f	NAC	26-01-22	17-02-22	09-05-22	-	-	-
437	m	NAC	26-01-22	17-02-22				
438	m	NAC	26-01-22	17-02-22	05-05-22	0.3254	54	99.6
488	f	NAC	16-02-22	09-03-22				
489	f	NAC	13-02-22	09-03-22				
490	f	NAC	16-02-22	09-03-22	18-05-22	0.5324	-	-
551	m	NAC	28-03-22	19-04-22				
553	m	NAC	28-03-22	03-05-22				
597	f	NAC	11-04-22	03-05-22				
599	f	NAC	11-04-22	16-12-21				
358	f	Control	02-12-21	23-12-21	14-04-22	0.7874	116	-
359	f	Control	02-12-21	23-12-21	22-03-22	1.2824	244	99.5
432	f	Control	26-01-22	17-02-22	14-04-22	0.7123	118	-
433	f	Control	26-01-22	17-02-22				
457	m	Control	11-02-22	04-03-22				
458	m	Control	11-02-22	04-03-22				
491	f	Control	16-02-22	09-03-22				
492	f	Control	16-02-22	09-03-22				
494	f	Control	16-02-22	09-03-22				
548	m	Control	28-03-22	19-04-22				
558	m	Control	28-03-22	19-04-22				
552	f	Control	28-03-22	19-04-22				
554	f	Control	28-03-22	19-04-22				

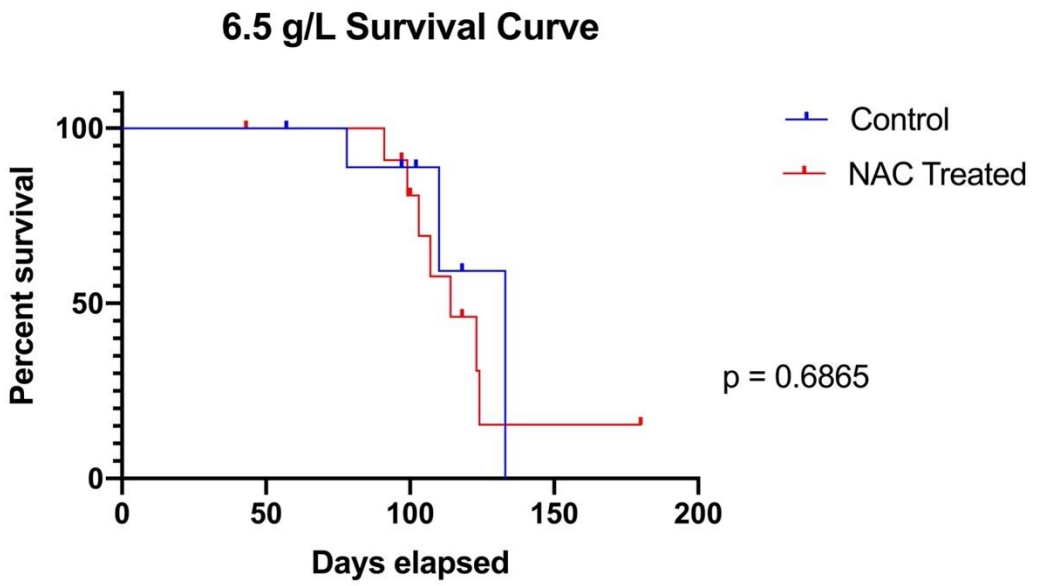

Figure 19. Mice administered 6.5 g/L of NAC through drinking water did not display an increase in survival compared to mice fed control water.

Kaplan-Meier survival curves of Mb1-CreΔPB mice administered either 1g/L NAC increased to 6.5 g/L according to the treatment schedule above in drinking water or regular reverse-osmosis tap water starting at day 21 of age. Mice on both treatment water had a median time to euthanasia of 15.79 weeks, and those and control water had a median time to euthanasia of 15.71 weeks. Log-rank (Mantel-Cox) test, control n = 13, NAC n = 15, p = 0.6865. 8 treatment mice and 10 control mice currently remain on the study.

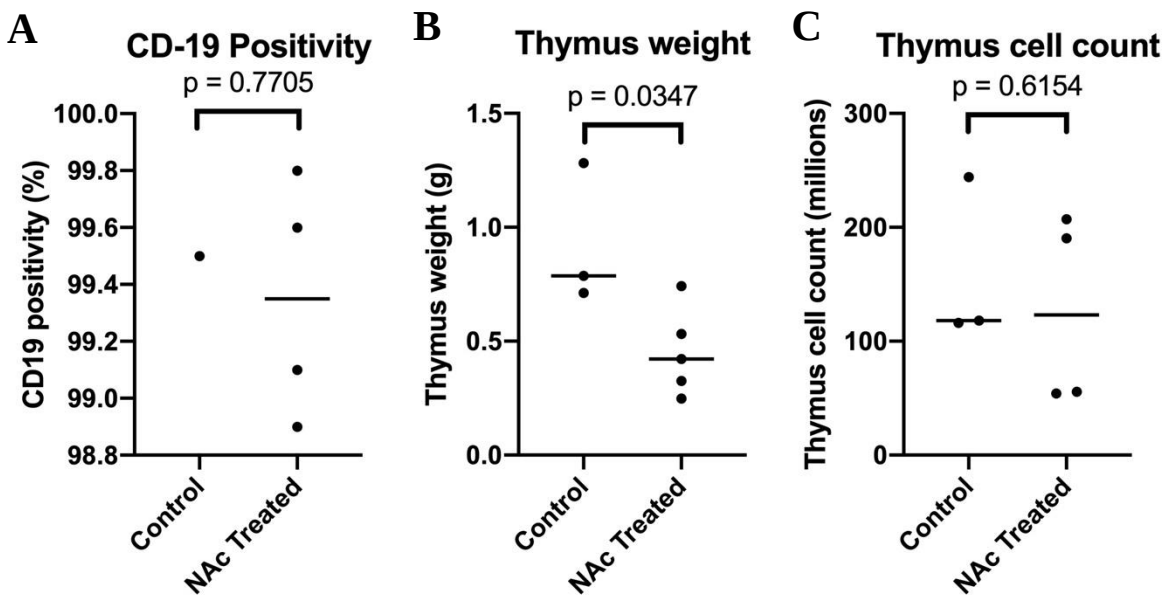

Figure 20. 6.5g/L NAC-treated mice have significantly lighter thymuses at time of euthanasia compared to control mice, whereas there is no significant difference in thymus CD19 positivity or thymus cell count.

CD19 positivity, thymus weight, and thymus cell count from Mb1-CreΔPB mice fed either control or 6.5g/L NAC water. **A)** CD19 positivity unpaired t test, control n = 1, NAC n = 4, p = 0.7705. **B)** Thymus weight unpaired t test, control n = 3, NAC n = 4, p = 0.0347. **C)** Thymus cell count unpaired t test, control n = 3, NAC n = 4, p = 0.6154.

3.8 Leukemias from mice on NAC and control water have significant differences in gene expression

A subset of mice from the 1g/L trial (8 treatment and 8 control) had RNA prepared from their thymuses, containing >99% CD19+ leukemia cells. Library construction and paired-end Illumina RNA-sequencing was performed by Genome Quebec. The resultant FASTQ files were analyzed on the usegalaxy.org platform using Salmon and DESeq2 programs to determine counts of each mRNA transcript from annotated genes in TPM (transcripts per million) and to determine genes that were differentially expressed between groups. One control sample (mouse 597) was excluded from statistical analysis because its mRNA expression profile did not match the other leukemias **(Figure 21)**, and had abnormally low CD19 positivity in the thymus, indicating that this mouse was potentially sick with something other than B-ALL at the time of euthanasia.

Using DESeq2 software, 254 genes were identified as being differentially expressed between treatment groups. An expression heat map showing the top 50 features of each treatment group indicates that there were substantial biological differences between groups (**Figure 22**). To identify specific pathways that were affected by NAC treatment, using the DAVID bioinformatics database, 5 KEGG (Kyoto Encyclopedia of Genes and Genomes) pathways were determined to have >4.5% of their genes included in the list of differentially expressed genes with a p value < 0.05. These pathways included the T cell receptor signaling pathways (6.2%, p=1.1e-10) **(Figure 23)**, cytokine-cytokine receptor interaction (6.2%, p=2.4e-5), human T cell leukemia virus 1 infection (4.9%, p=5.3e-4), calcium signaling pathway (4.5%, p=1.6e-3) **(Figure 24)**, and pathways in cancer (5.4%, p=4.4e-2) **(Figure 25)**.

The T cell receptor signaling pathway included the highest percentage of genes identified as differentially expressed as well as the lowest p-value, so this pathway was selected for further analysis. Gene set enrichment analysis (GSEA) designated a marked downregulation of these genes in the NAC group, however, the heatmap showed that essentially only one mouse (593) in the control group was responsible for this difference and was not an overall difference between the two groups **(Figure 26)**.

The calcium signaling pathway was also identified as a significantly differentially expressed pathway by DAVID. The top two genes identified by DESeq2 were *Plcb2* and *Plcb4* (encoding phospholipase C beta 2 and 4), which are implicated in calcium signaling and therefore this pathway was also selected for further analysis. Through GSEA, the entire calcium signaling pathway was not shown to be differentially regulated between NAC and control mice, however, selection of genes only involved in calcium signaling between the endoplasmic reticulum and mitochondria to regulate apoptosis in high ROS concentrations indicated a clear dissimilarity between the two groups **(Figure 27A)**, with genes such as *Pten* and *Bmf* overexpressed in NAC mice and genes including *Bcl2*, *Plcb2*, and *Plcb4* being underexpressed **(Figure 27B and C)**. In this pathway, a ligand binding to its G protein coupled receptor triggers a cascade of events lead by the activation of phospholipase C proteins. These enzymes catalyze the hydrolysis of PIP2 (phosphatidylinositol 4,5-bisphosphate) to IP3 (inositol 1,4,5-triphosphate) and DAG (diacylglycerol). IP3 activates its receptors triggering release of calcium ions from the endoplasmic reticulum directly into adjacent mitochondrial calcium importers. High levels of calcium in the mitochondria triggers apoptosis through cytochrome C release into the cytoplasm. This process is inhibited by Bcl2 and is activated by Pten and BMF. A simplified schematic of the major proteins involved in this pathway is shown in **Figure 28**.

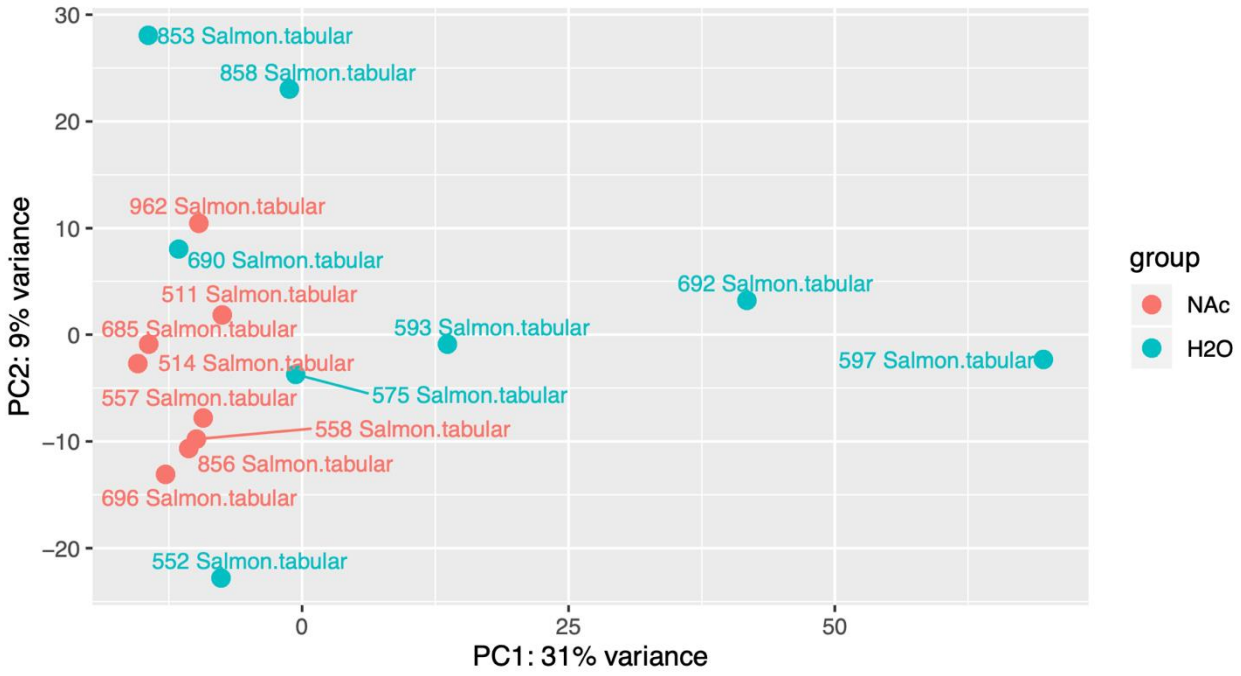

Figure 21. Principal component evaluation of differential expression analysis of Mb1-CreΔPB tumours.

N-acetylcysteine-treated mice are clustered on the left side whereas control mice are spread on the x- and y-axis. Clustering of samples indicates similarity in terms of gene expression.

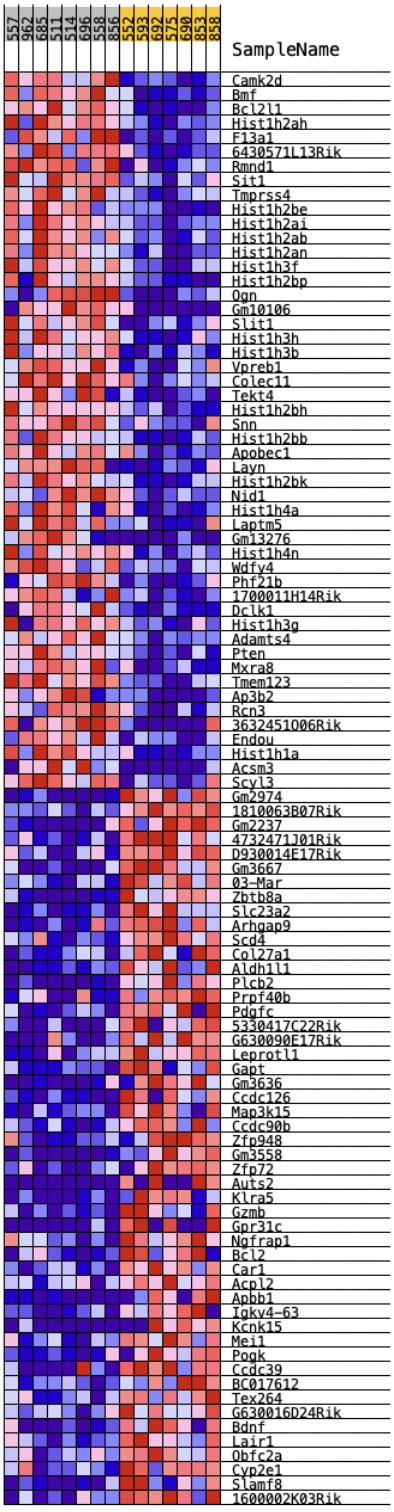

Figure 22. Heatmap of the top 50 features of each treatment group in terms of expression.

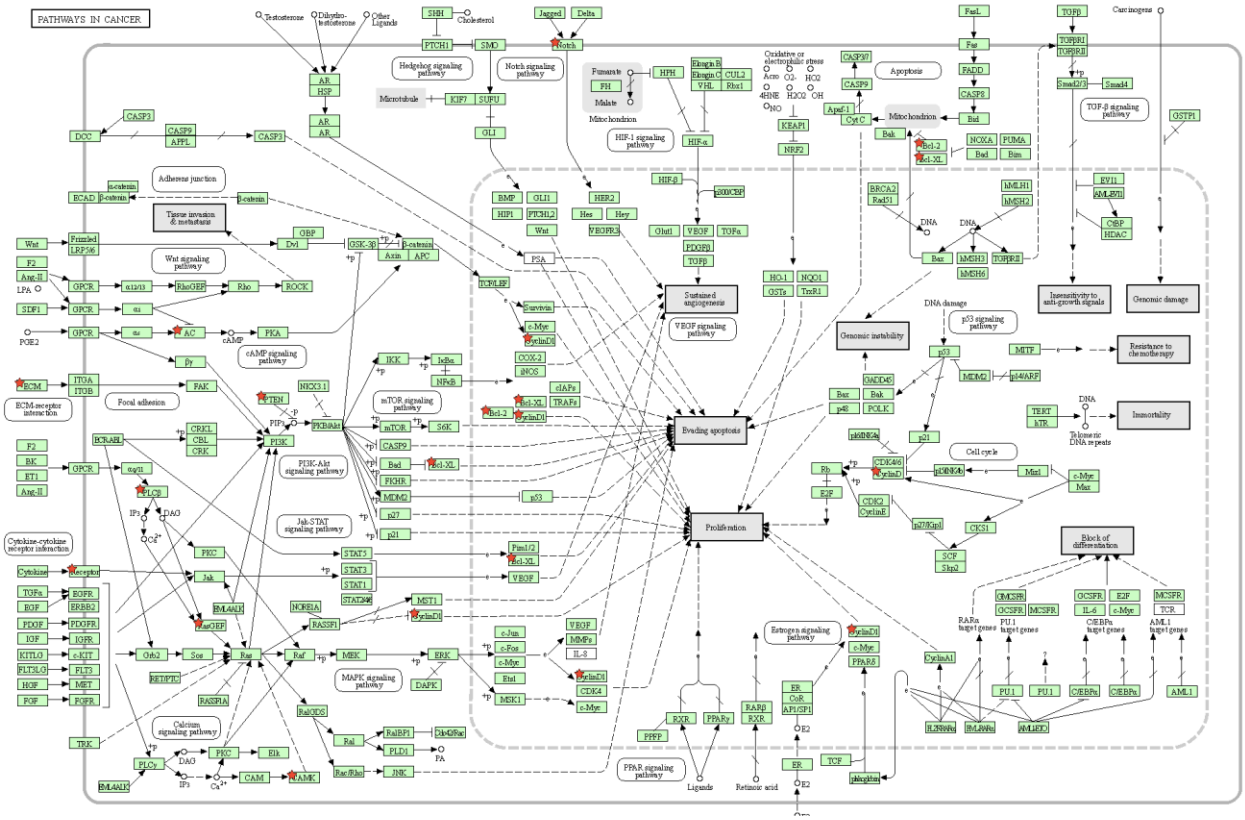

Figure 23. DAVID pathway analysis of the KEGG gene-set "Pathways in Cancer".

Genes starred with red indicate genes that were differentially expressed between NAC-treated and control water mice.

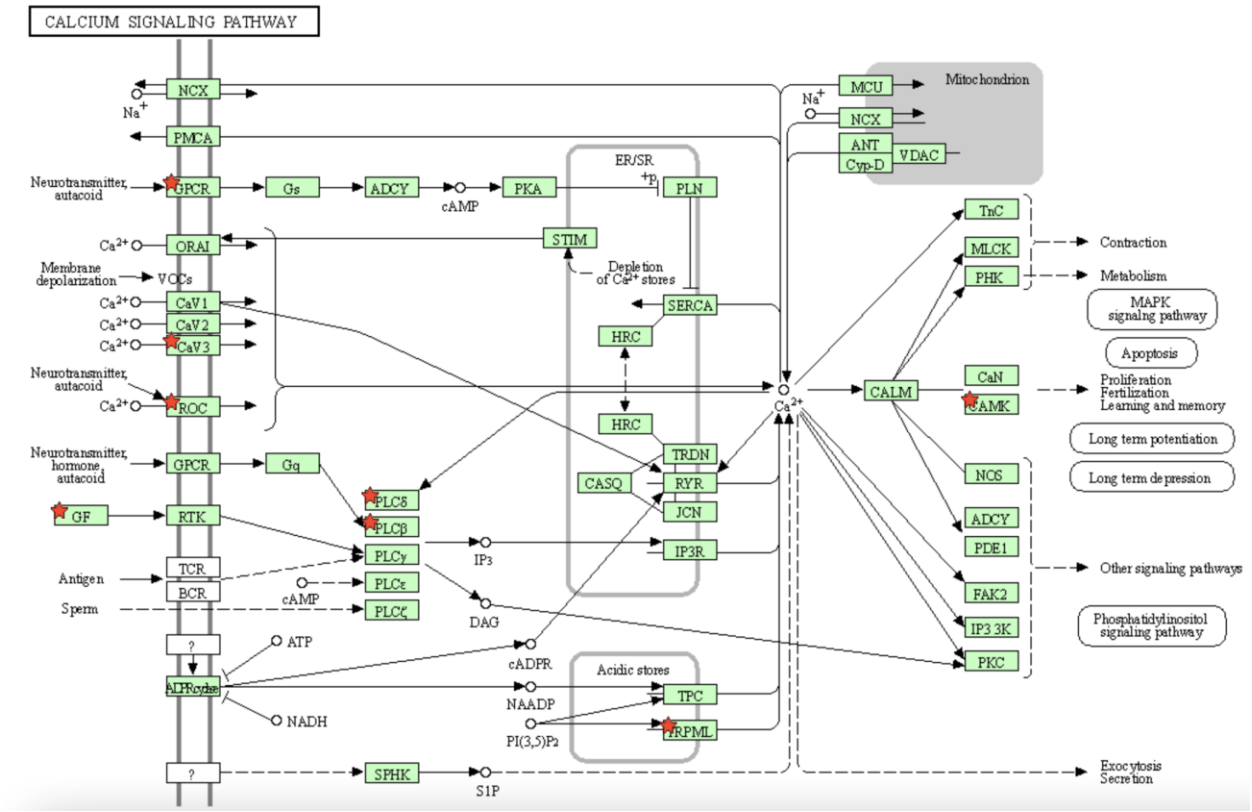

Figure 24. DAVID pathway analysis of the KEGG gene-set "Calcium Signaling Pathway".

Genes starred with red indicate genes that were differentially expressed between NAC-treated and control water mice.

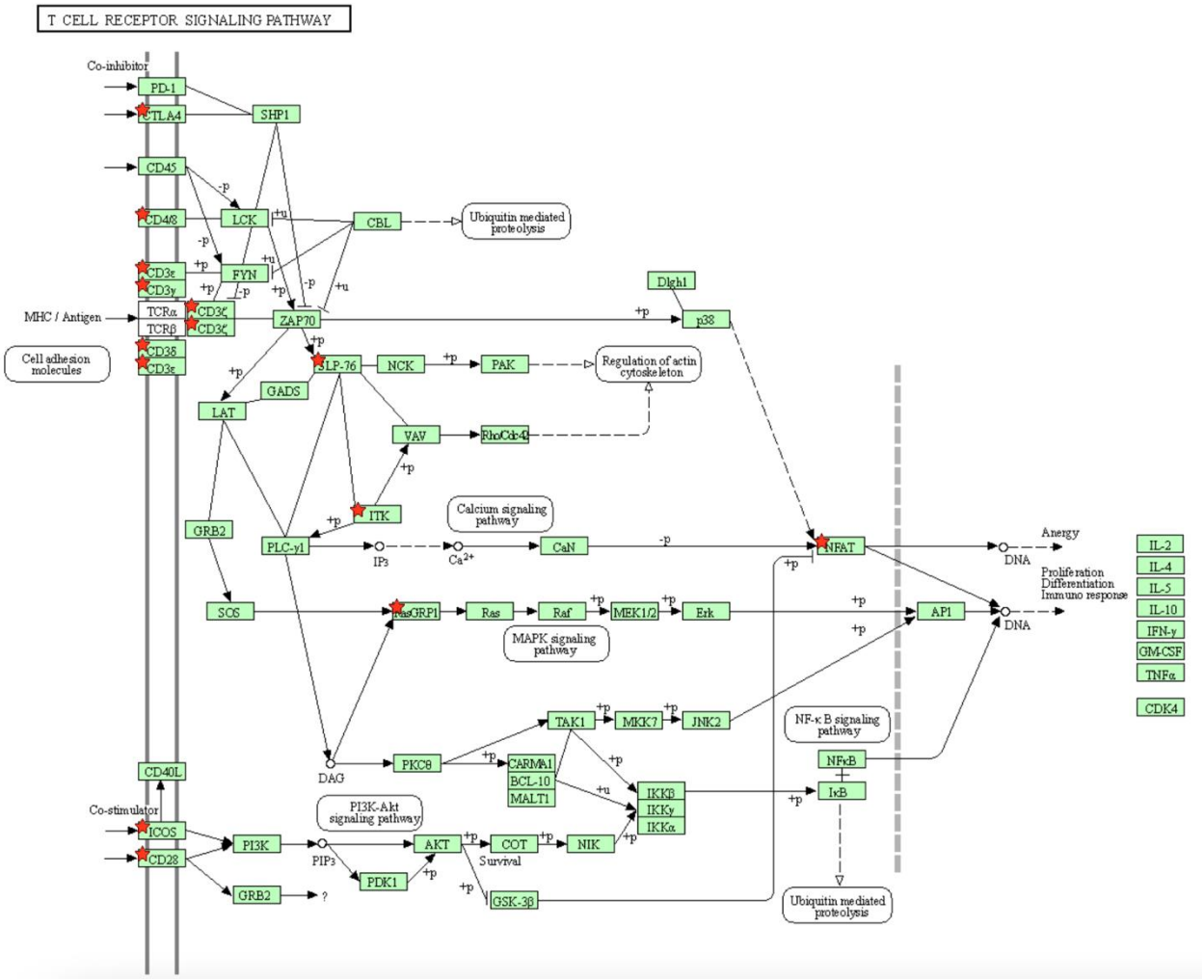

Figure 25. DAVID pathway analysis of the KEGG gene-set "T cell Receptor Signaling Pathway".

Genes starred with red indicate genes that were differentially expressed between NAC-treated and control water mice.

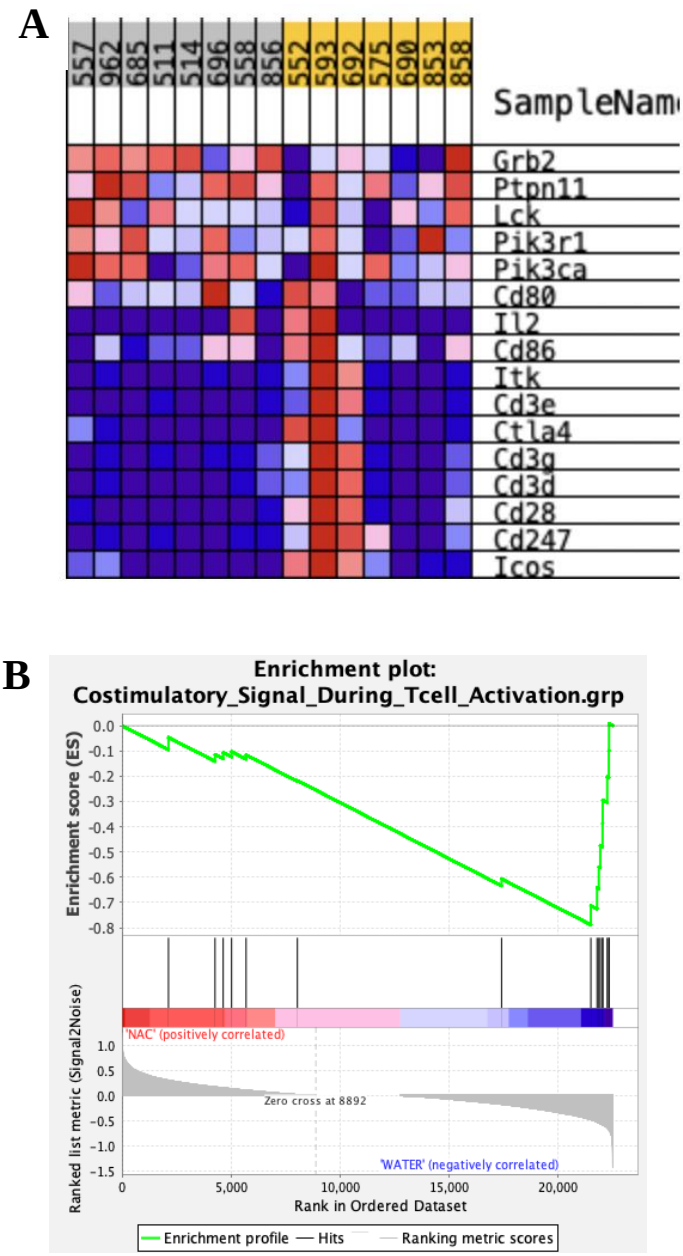

Figure 26. The effect of NAC on expression genes involved in T cell activation in Mb1-CreΔPB mice.

A) Heat map of gene expression in Mb1-CreΔPB mice either fed control 1g/L N-acetylcysteine (557, 962, 685, 511, 514, 696, 558, 856) or control water (552, 593, 692, 575, 690, 853, 858). Darker blue indicates low expression, while dark red indicates high expression. **B)** Gene set enrichment analysis of expression of the same genes listed in the heat map. Normalized enrichment score (NES) = -1.296147, FDR q value = 0.06105263.

A

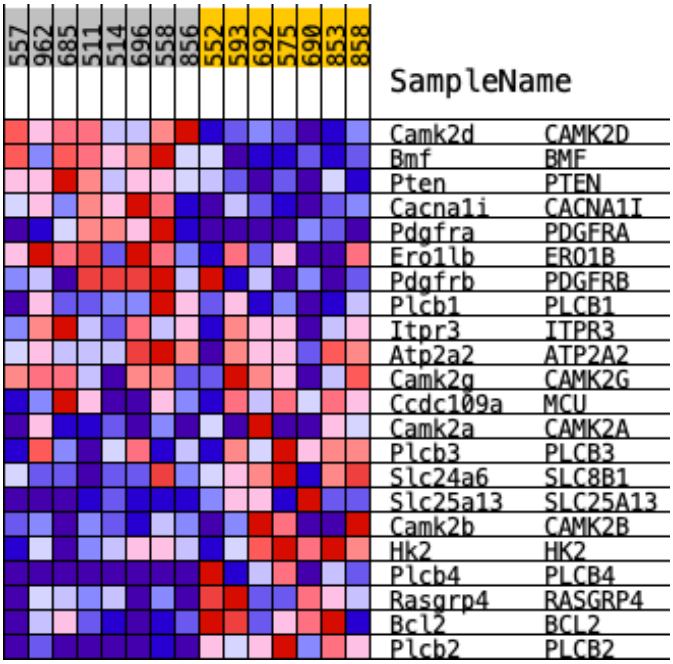
557
962
685
511
514
696
558
856
552
593
692
575
690
853
858
SampleName
Camk2d CAMK2D
Bmf BMF
Pten PTEN
Cacna1i CACNA1I
Pdgfra PDGFRA
Ero1lb ERO1B
Pdgfrb PDGFRB
Plcb1 PLCB1
Itpr3 ITPR3
Atp2a2 ATP2A2
Camk2g CAMK2G
Ccdc109a MCU
Camk2a CAMK2A
Plcb3 PLCB3
Slc24a6 SLC8B1
Slc25a13 SLC25A13
Camk2b CAMK2B
Hk2 HK2
Plcb4 PLCB4
Rasgrp4 RASGRP4
Bcl2 BCL2
Plcb2 PLCB2

B

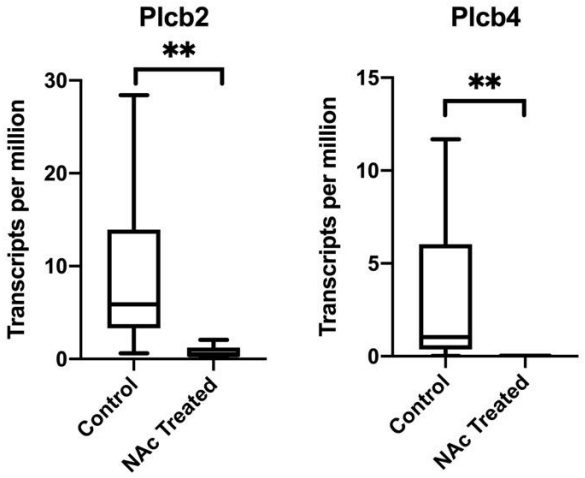
Plcb2
**
Transcripts per million
30
20
10
0
Control
NAc Treated
Plcb4
**
Transcripts per million
15
10
5
0
Control
NAc Treated

C

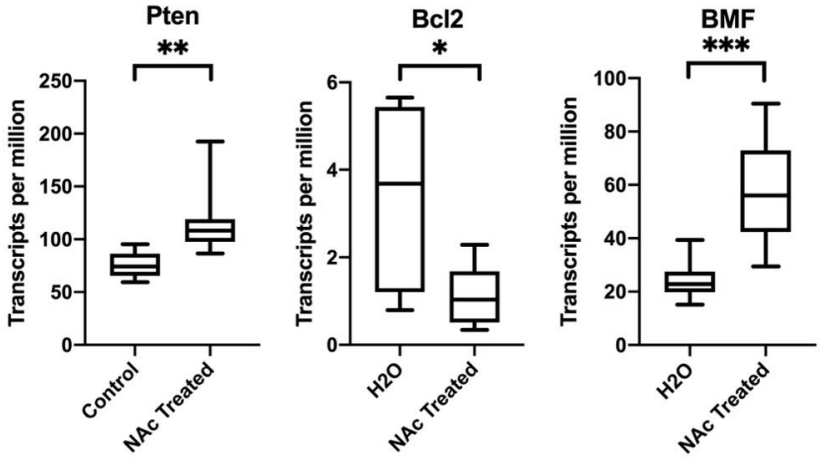
Pten
**
Transcripts per million
250
200
150
100
50
0
Control
NAc Treated
Bcl2
*
Transcripts per million
6
4
2
0
H2O
NAc Treated
BMF
***
Transcripts per million
100
80
60
40
20
0
H2O
NAc Treated

Figure 27. The effect of NAC on expression of genes involved in calcium regulation of apoptotic signals in the endoplasmic reticulum and mitochondria in Mb1-CreΔPB mice.

A) Heatmap of gene expression in Mb1-CreΔPB mice either fed control 1g/L N-acetylcysteine (557, 962, 685, 511, 514, 696, 558, 856) or control water (552, 593, 692, 575, 690, 853, 858). Darker blue indicates low expression, while dark red indicates high expression. **B)** Raw TPM counts of the two most differentially expressed genes identified by DESeq2, Phospholipase C Beta 2, and Phospholipase C Beta 4. Both Plcb2 and Plcb4 have significantly reduced expressed in the NAC group. Mann-Whitney tests Plcb2 $p = 0.0012$, Plcb4 $p = 0.0037$. **C)** Raw TPM counts of tumour suppressor gene Pten, the oncogene Bcl2 and Bcl2-modifying factor gene BMF. Mann-Whitney tests Pten $p = 0.0012$, Bcl2 $p = 0.0205$, BMF $p = 0.0006$.

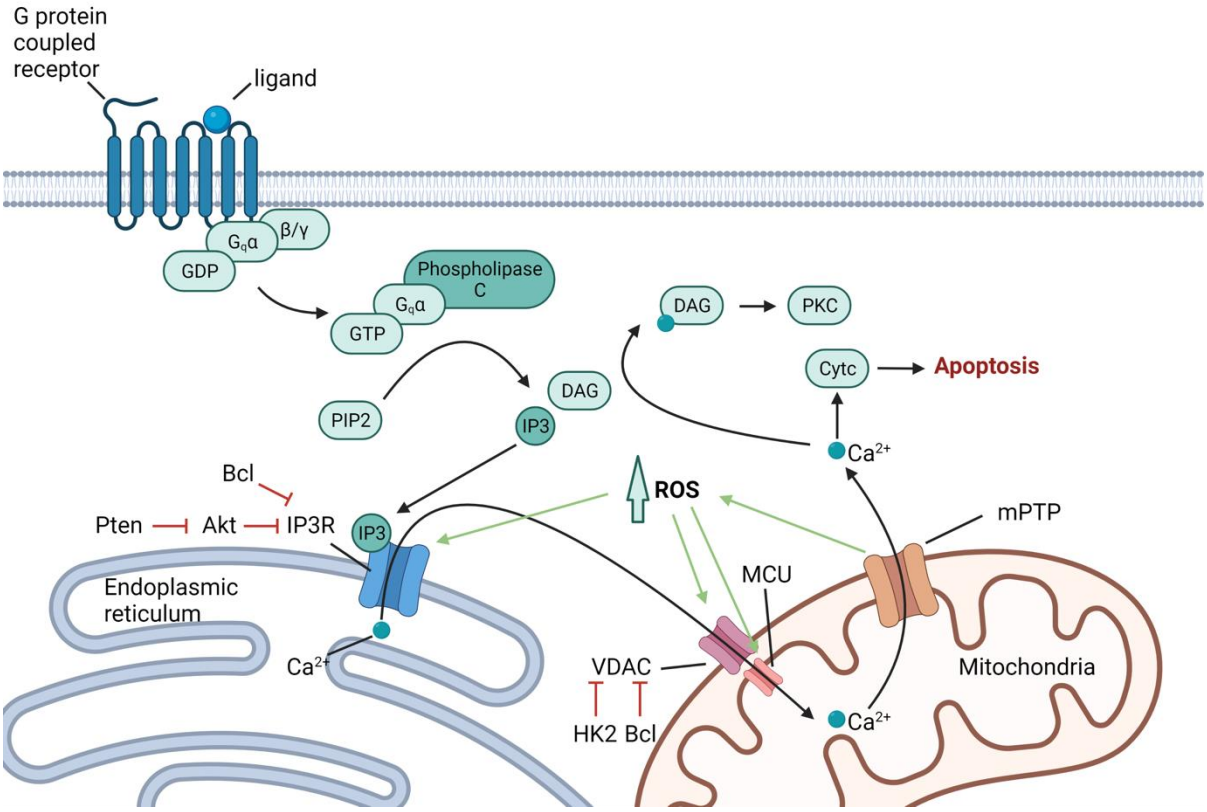

Figure 28. Simplified schematic of the proposed calcium signaling pathway affected by NAC treatment.

When a ligand binds its G protein coupled receptor (GPCR), intracellular GDP is switched for GTP and the alpha unit of the GPCR along with GTP is transferred onto a phospholipase C (for example, Plcb2 or Plcb4). Activated phospholipase C catalyzes the conversion of PIP2 to IP3 and DAG. IP3 activates the IP3 receptor (IP3R) on the membrane of the endoplasmic reticulum, allowing calcium to move from the endoplasmic reticulum to the mitochondria through the IP3R, VDAC and MCU channels. Excess calcium in the mitochondria begins a cascade that allows calcium to leak into the cytoplasm, signalling apoptosis through cytochrome C (Cytc).

3.9 Genes involved in somatic hypermutation and class-switch recombination of the B cell receptor are differently expressed between treatment and control mice

The combination of Rag1/Rag2 and AID are known to be essential for somatic hypermutation and class-switch recombination that occurs during the development of the B cell receptor (Wu *et al.* 2003). *Rag1* and *Rag2* are preferentially expressed in early B cell development whereas *Aicda* (encoding AID) is preferentially expressed at later stages after antigen encounter. *Aicda* had significantly higher levels of expression in NAC-treated mice, whereas both *Rag1* and *Rag2* had higher levels of expression in control mice, though not significant **(Figure 29)**. Aberrant upregulation of *Aicda* is common in this leukemia model (Lim *et al.* 2020).

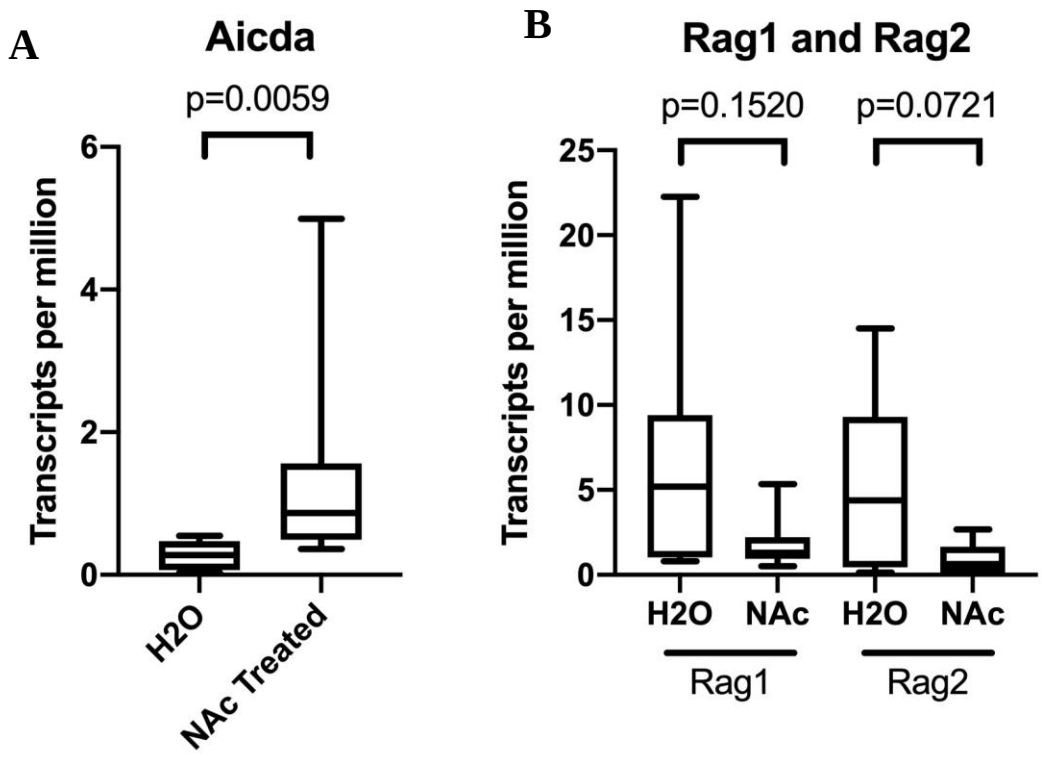

Figure 29. Gene expression of *Aicda* and *Rag1/2* in NAC-treated and control mice

A) *Aicda* is expressed significantly higher in NAC-treated mice. Mann-Whitney test. **B)** Both *Rag1* and *Rag2* are expressed at higher levels in control mice compared to NAC-treated mice. Mann-Whitney tests.

3.10 Leukemic mice have high mutation frequency in Ikzf3, Jak1, Jak3, Trp53, and Sf3b1

Single nucleotide variants were manually discovered using the Integrated Genome Viewer (IGV) software. Genes of interest were selected based upon mutations found previously in our lab, known mutations in pre-B-ALL, and tumour suppressors and oncogenes. Mutations were considered present in nucleotides that had >500 reads and in which the mutant was present in >5% of the reads (**Figure 30**). A summary of the mutations observed can be found in **Figure 31A**. 5 different mutations were observed in *Jak1*, 4 of which are located in the autoinhibitory pseudokinase region and the remaining being found between the SH2 and pseudokinase region (**Figure 31B**). One recurrent mutation was observed in the pseudokinase region of *Jak3*, R653H, which was found in 6/8 NAC-treated mice and 2/7 control mice. NAC treated mice were both more likely to harbour this R653H mutation, and in those mice that did harbour the mutation, NAC mice had a higher variant allele frequency (**Figure 31C**). Interestingly, of the two NAC mice that did not harbour the *Jak3* R653H mutation, these were the only two mice with *Jak1* mutations. 11 different mutations were observed in *Ikzf3*, mostly concentrated within the zinc finger domains, including a variety of truncation mutations which were not observed in any of the other genes investigated (**Figure 31B**). Two recurrent mutations were observed in *Trp53* encoding the oncogene p53 in adjacent nucleotides although the variant allele frequency was similar among all mice harbouring these mutations. One recurrent mutation was observed in *Sf3b1*, a commonly mutated gene in cancer, which, when mutated incorrectly splices proteins that have been shown to drive cancer (Inoue *et al.* 2019). This mutation also had similar variant allele frequency among all mice.

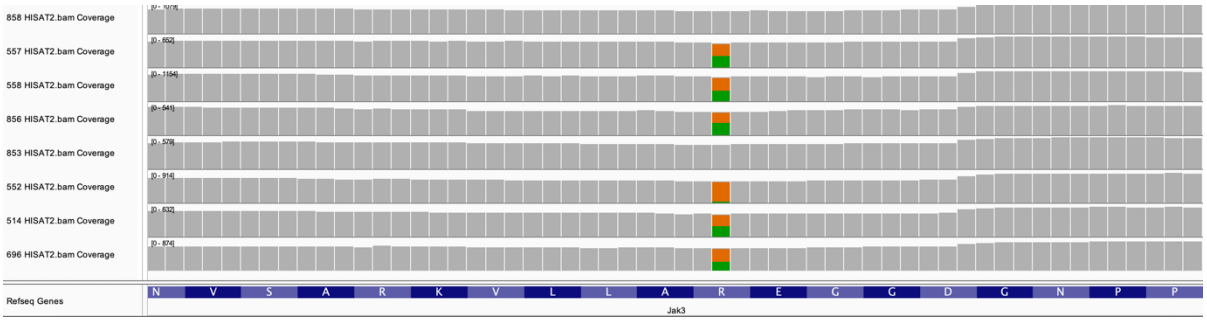

Figure 30. A representative screenshot of the IGV output for the *Jak3* R653H mutation.

Mouse identities are listed on the left and each nucleotide is represented by a grey bar. Bars were selected to be highlighted in colour if a mutant allele was read at a frequency of 0.05 or higher. The orange section of the bar represents the correct nucleotide for that position, G, and the green section represents the frequency of the mutant nucleotide, A.

A

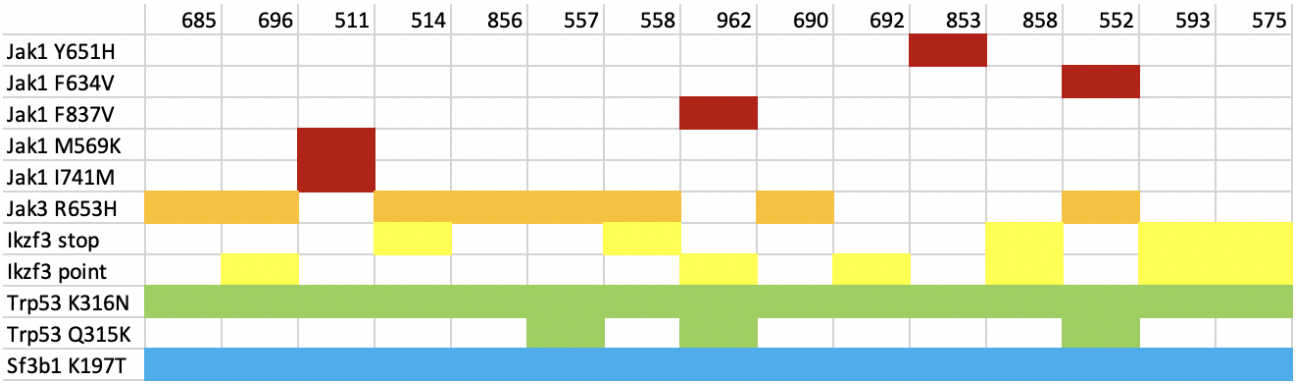
685
696
511
514
856
557
558
962
690
692
853
858
552
593
575
Jak1 Y651H
Jak1 F634V
Jak1 F837V
Jak1 M569K
Jak1 I741M
Jak3 R653H
Ikzf3 stop
Ikzf3 point
Trp53 K316N
Trp53 Q315K
Sf3b1 K197T

B

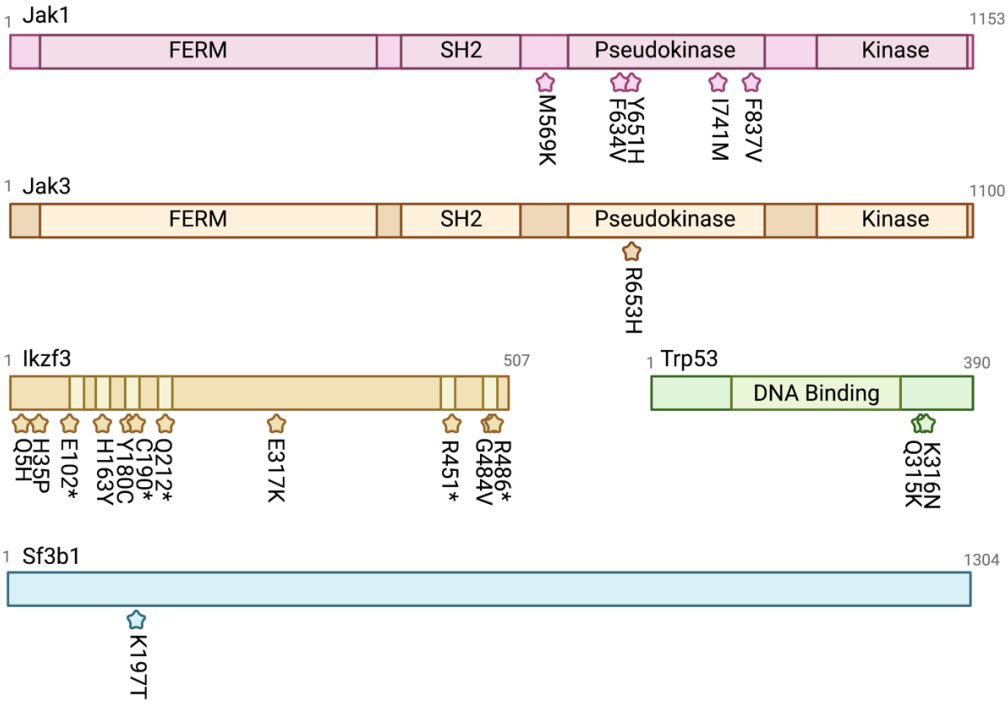
Jak1
1
1153
FERM
SH2
Pseudokinase
Kinase
M569K
Y651H
F634V
I741M
F837V
Jak3
1
1100
FERM
SH2
Pseudokinase
Kinase
R653H
Ikzf3
1
507
H35P
Q5H
E102*
H163Y
Y180C
C190*
Q212*
E317K
R451*
R486*
G484V
Trp53
1
390
DNA Binding
K316N
Q315K
Sf3b1
1
1304
K197T

C

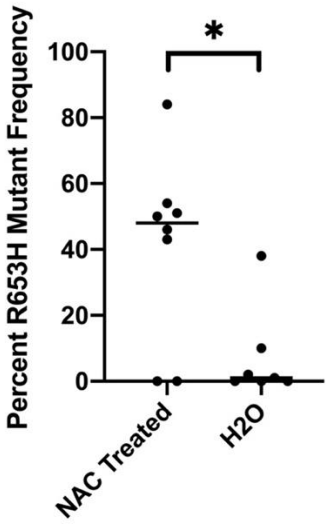
*
100
80
60
40
20
0
Percent R653H Mutant Frequency
NAC Treated
H2O

Figure 31. Identified mutations in conserved regions of Jak1, Jak3, Ikzf3, Trp53, and Sf3b1 genes.

A) Summary of all point mutations found in manual screening of Jak1, Jak3, Ikzf3, Trp53, and Sf3b1 from a panel of leukemias taken from N-acetylcysteine-treated mice (685, 696, 511, 514, 856, 557, 558, and 962), and control mice (690, 692, 853, 858, 552, 593, and 575). A variety of Jak1 and Ikzf3 mutations were identified, including multiple truncating mutations in Ikzf3. Jak3 R653H was found in 6/8 N-Acetylcysteine leukemias and 2/7 control leukemias. Trp53K316N and Sf3b1K197T were found in all leukemias and an additional Trp53 mutation (Q315K) was found in 3/15 leukemias. **B)** Schematic of the Jak1, Jak3, Ikzf3, Trp53, and Sf3b1 proteins including their important functional domains with identified amino acid substitutions indicated with stars. Domains in Jak1 and Jak3 include 4.1 protein, exrin, radixin, moesin (FERM), Src homology 2 (SH2), pseudokinase, and kinase. Ikzf3 domains include 4 zinc finger DNA binding domains at the N terminus and 2 zinc finger dimerization domains near the C terminus. Trp53 includes one large DNA binding domain. Sf3b1 does not have any identified specific functional domains. **C)** Percent frequency of the R653H Jak3 mutation in all 15 RNA sequencing samples. This mutation is found in significantly more cells in the NAC-treated group compared to the control group.

Chapter 4

4 Discussion

Taken together, the results presented in this thesis suggest that 1g/L of NAC administered through drinking water to Mb1-CreΔPB mice does not confer an increase in survival but does significantly change the biology of the tumours that eventually form. The tumours found in NAC mice have different gene expression signatures in several genes, specifically those from the calcium/apoptosis regulation pathway and in genes involved in typical B cell development. From preliminary data, the mutation signatures found within the tumours are also different between treated and control mice. At 11 weeks, 1g/L of NAC was found to have delayed onset of leukemogenesis but these mice end up reaching sickness at the same time as their control counterparts who start developing tumours earlier on in life. This suggests that the tumours found in NAC-treated mice are more aggressive at the time of euthanasia.

4.1 Differences in dose per gram of body weight affected survival of Mb1-CreΔPB mice receiving 1g/L N-acetylcysteine

In the initial 1g/L trial, female mice receiving N-acetylcysteine were observed to have slightly better, although non-significant survival over control mice when compared to male mice. While this difference was small, it prompted an investigation into what biological differences between male and female mice could account for this difference. Disparities in weight between male and female mice were large enough that it could conceivably cause large differences in NAC dose per body weight received. This could account for the difference in survival seen between NAC female mice and NAC male mice.

Additionally, when NAC female mice were split up based on length of survival, an unpaired t test showed that the mice that survived the longest were those that weighed the least. Importantly, this difference in weight was not only visible near the end of life, but throughout the entire lifespan starting at day 21 when the mice were first weighed. Near

end-of-life, factors such as fewer mice alive contributing to weight averages, and lost weight due to sickness can skew weight data, but the initial large portion of life still showed a clear disparity in weight based on survival. This data also supports the conclusion that 1g/L of N-acetylcysteine affects mice differentially based on their dose per gram of body weight.

However, the preliminary data presented from the 6.5g/L NAC trial contradicts this hypothesis, with the heightened dose still not conferring an increase in survival. In hindsight, a 650% increase in dosage for a 25% difference in observed weights may have induced either increased effects of worsening tumour progression or toxicity that skewed the results from what was predicted. An additional dosing experiment testing multiple intermediate doses with smaller cohorts of mice may elucidate an optimal dosage for future experiments.

Lastly, before additional experiments are designed, an investigation into disease-specific survival versus overall survival must be conducted. As previously mentioned, some mice were removed from other statistical analyses due to evidence that the cause of death was not leukemia. To account for these deaths, disease-specific survival would be an additional appropriate measure to investigate how NAC is affecting leukemic progression.

4.2 Leukemia progression occurs rapidly and may be postponed, but accelerated by N-acetylcysteine administration

11 weeks was chosen as an intermediate timepoint based on our lab's previous work that showed that leukemia cells were detectable in the thymus of Mb1-CreΔPB mice at 11 weeks. At 11 weeks, most litter pairs had similar CD19 levels, with either both mice having low (<15%) or high (>80%) CD19 positivity indicating healthy thymus or fully leukemic thymus, respectively. Importantly, only two mice out of the 16 total were caught at an intermediate level of tumour progression, both with their litter mate having low to no tumour progression. Taken together, these results indicate that the mice progress from very low CD19 frequency to very high CD19 frequency in the thymus

within a relatively short timeframe, and that mice within the same litter would not likely be at vastly different points in their leukemic progression at the same time point. Importantly, these moderate CD19 frequencies were not observed in any of the sickness-as-endpoint trials, suggesting that it represents an intermediate stage of both B cell infiltration to the thymus and leukemia progression.

The observation that none of the N-acetylcysteine-treated mice displayed high CD19 positivity at 11 weeks after receiving 1g/L doses, but that there was ultimately no survival difference between treated and control mice at 1g/L, suggests that the tumours observed in the treated mice were initiated later in life but progressed more rapidly. Interestingly, many of the control mice had high tumour progression at the 11-week timepoint, but only three control mice out of 15 were euthanized before 14 weeks of age, indicating that the mice can survive without signs of illness for long after the tumour has significantly advanced. This may not be the same for N-acetylcysteine-treated mice, in which tumour initiation is significantly delayed but sickness and death is not. This suggests that the addition of 1 g/L of N-acetylcysteine causes faster onset of physical symptoms from start of B cell infiltration into the thymus.

A potential mechanism for this phenomenon is the increase in expression of *Aicda* in N-acetylcysteine-treated mice. Whole exome sequencing performed by our lab suggested AID and ROS as two independent sources of secondary driver mutations in B-ALL, with those caused by AID hypothesized to be occurring earlier on in clonal evolution. The small, but observable, increase in *Aicda* expression in N-acetylcysteine-treated mice may be responsible for the delayed progression but increased aggressiveness of these leukemia clones.

Furthermore, in the mice receiving 6.5 g/L NAC, lighter thymuses were observed compared to control counterparts. Typically, the signs of illness in Mb1-CreΔPB mice are due to an inability to efficiently breathe with a large tumour occupying the chest cavity, presenting as laboured breathing and a hunched appearance. However, the NAC-treated mice presented with these symptoms albeit with a mean thymus weight of less than half of the mean thymus weight in the control group. This suggests that the NAC tumours are

more aggressive in that they confer physical symptoms of sickness long before the mere size of the tumour would impede breathing ability.

4.3 Wider variation in gene expression in control mice may be due to accumulation of driver mutations late in clonal evolution

As noted in the introduction, whole exome sequencing of Mb1-CreΔPB tumours suggested that ROS is responsible for introducing secondary driver mutations late in clonal evolution. Principal component analysis of mRNA counts within these tumours demonstrated a wide variation between control mice, whereas N-acetylcysteine-treated mice tend to be more tightly clustered around the origin. Mutations occurring during mid- to late-leukemic progression would result in an increased number of clones within the tumour, potentially preferentially expressing different genes.

When showing a difference between two treatment groups, ideally the two groups would separate along the x-axis of a principal component analysis. However, the N-acetylcysteine-treated mice are clustered on the left of the x axis, while the control mice are spread along both the x axis and the y axis. This indicates that the control mice are not what would typically be considered sample ‘replicates’ as they display a large amount of variation. This would be explained by differing leukemic clones being analyzed for gene expression in each mouse, which would reasonably be created by a substantial amount of late-clonal evolution mutations. Higher levels of ROS would be expected to create more late-clonal evolution mutations and therefore higher gene expression variability.

In addition, the control mice in the 11-week trial displayed much greater variability in CD19 positivity and thymus weight when compared to treatment mice, with similar variability between the groups in thymus cell count. When observing CD19 positivity, the N-acetylcysteine treated mice tend to cluster around the low CD19 bin with only one exception, whereas the control mice are spread across all three bins (low, mid, and high CD19 positivity).

4.4 Evidence for physiological differences between cells in N-acetylcysteine and control mouse thymuses

The three mice that had low CD19 positivity in the 11-week control cohort had the highest thymus cell counts while the four mice with the highest CD19 positivity had the lowest cell counts in their respective groups. This points to a potential association between tumour progression and therefore thymus overall health, and total cell numbers within the thymus. There is also a clear correlation between thymus cell count to weight ratio and CD19 positivity, indicating that healthier thymuses with less B cell infiltration tend to have higher cell counts with lower thymus weights.

The main function of a healthy thymus is to facilitate maturation of T lymphocytes and provides a location for positive and negative selection of autoreactive T cells. A mouse thymus generates many new thymocytes daily, but a very small proportion of those survive positive and negative selection and exit the thymus as mature T cells (Klein *et al.* 2014). A typical mouse thymus contains around $2\mathbf{x10}^{8}$ thymocytes at any given time. Mb1-CreΔPB tumours are comprised of large pre-B cells which represent a stage of B cell development that has larger volume cells, and the term “blastic” in lymphoblastic leukemia signifies the large size of these cancerous cells. Additionally, thymic T cells undergoing selection would likely not be in S or G_2 phases of the cell cycle, whereas a large population of tumour cells would be expected to be in these phases of replication, resulting in a large average cell size within a large pre-B cell tumour compared to a T cell-containing thymus. This supports the hypothesis that high thymus cell count to weight ratio is indicative of a healthier thymus.

In the litter-matched 11-week mice, all four thymuses were roughly the same size, indicating that the differences observed in weight and cell count were due to physiological and potential cell-type differences within the tumor, rather than a simple enlargement or shrinking of thymic tissue. Supplementary to cell size, colour of thymus tissue varied between control and treatment mice. Control thymuses appeared much redder in colour compared to NAC thymuses at the 11-week timepoint. One of the hallmarks of cancer is high vascularity, which is due to rapid development of new blood vessels, and high requirements for blood flow providing nutrients and oxygen to rapidly

dividing cells resulting in a redder appearance of tissue (Hanahan 2022). In contrast, the mice receiving 1g/L NAC and euthanized at sickness had significantly increased expression of the endothelial cell marker CD31, indicating increased vascularity within these tumours. This suggests that at 11 weeks, NAC mice have lower thymus vascularity compared to control mice but rapidly build up the vascularity as the tumours progress to surpass control tumour progression. In the future, immunohistochemistry against CD31 on sections of tumour tissue can verify these findings.

4.5 Calcium signaling for apoptosis is a candidate pathway affected by NAC treatment

Through RNA sequencing gene expression analysis, the calcium-apoptosis signaling pathway was determined to be differentially expressed between NAC treatment and control groups. Typically, GSEA analysis similar to the analysis shown for T cell activation is performed to conclude whether a pathway is considered differentially expressed. However, GSEA is intended for use on unidirectional gene sets, meaning that every gene in the set works to either activate or repress a pathway. In this case, genes that both activate and repress the calcium-apoptosis pathway are included in order to have a sufficient number of genes without including genes that are only peripherally related to the pathway. A clear pattern does emerge however, with approximately one third of the genes being highly expressed in NAC tumours and one half of the genes being highly expressed in control tumours.

Determining directionality in this pathway is not easily deduced, as genes that activate the pathway such as *Plcb2* and *Plcb4* acting to activate IP3R, incidentally the two most differentially expressed genes reported by DESeq2, are upregulated in control mice, but genes like *Bcl2* which inhibits the action of IP3R (Pinton and Rizzuto 2006) are also upregulated in control mice. Some of the genes clearly activating calcium movement into the mitochondria, signaling apoptosis are *Camk2d*, *Bmf*, *Pten*, *Pdgfrb*, *Plcb1-4*, *Itpr3*, and *Rasgrp4* (Hempel and Trebak 2017). The majority of these genes are upregulated in NAC-treated mice. Conversely, some of the genes involved in inhibiting this pro-apoptotic pathway are *Slc24a6*, *Hk2*, and *Bcl2* (Hempel and Trebak 2017), all of which are upregulated in control mice (**Figure 27**). These results suggest that tumour cells in

NAC mice have increased activation of pro-apoptotic signaling through the endoplasmic reticulum-mitochondria calcium release axis.

Interestingly, intracellular ROS levels tend to drive this pathway, so we would expect to see decreased calcium signaling in NAC-treated mice. The IP3R on the endoplasmic reticulum, mitochondrial voltage-dependent anion channel (VDAC) and mitochondrial Ca^{2+} uniporter (MCU) are activated through redox (Madesh and Hajnoczky 2001, Yan *et al.* 2008). Previous gene expression analysis of Mb1-CreΔPB tumours showed that many antioxidant genes were downregulated compared to control cells (Lim *et al*. 2020), but other tumour cells have been shown to increase expression of antioxidants, perhaps to adjust to high levels of ROS (Jaramillo and Zhang 2013). An increased level of antioxidants in cells that already have low antioxidant expression such as Mb1-CreΔPB tumours may provide the cells with an advantage in adjusting to rapidly changing ROS states throughout tumour progression. If NAC tumours are able to ameliorate high levels of ROS through scavenging mechanisms during their early stages of development to accumulate driver mutations through alternate processes such as overactive AID, they might become more aggressive near end-of-life, resulting in heightened apoptotic signaling at euthanasia when gene expression profiles are measured.

When PIP2 is not hydrolyzed by PLC enzymes, it may be phosphorylated by phosphoinositide 3-kinase (PI3K), which is a pathway implicated in the progression of ALL (Holmfeldt *et al.* 2013). Reduced expression of PLC in NAC-treated mice might increase the ability of PI3K to induce leukemic signaling. Other studies have shown that leukemic cell lines have reduced proliferation in the presence of PI3K inhibitors (Holmfeldt *et al.* 2013), suggesting that downstream effects of low PLC may contribute to the increased aggressiveness of the leukemias observed in NAC mice.

4.6 Mutations in Janus Kinases and Ikzf3 may act as driver mutations of leukemogenesis

Five distinct *Jak1* mutations were observed in this subset of mice, one of which has been previously identified by our lab, F837V (Lim *et al.* 2020). All these mutations except M569K were located within the autoregulatory pseudokinase domain and are thus

predicted to act as activating mutations (Morris *et al.* 2018). The recurrent *Jak3* R653H mutation, similarly located in the pseudokinase domain, has also been previously described by our lab and has been shown to act as an activating mutation involved in IL-7 signaling for pro-B cell proliferation (Batista *et al.* 2018). This mutation is postulated to be equivalent to the *Jak3* R657Q mutation observed in human ALL (Losdyck *et al.* 2015). 8/11 mutations in Ikzf3 were located in zinc finger domains either used to bind DNA or dimerize and are therefore expected to function as loss-of-function mutations (Rebollo and Schmitt 2003). The H163Y mutation located in the second DNA-binding zinc finger is also found in the highly related *Ikzf1* gene in which the mutation completely abolished DNA binding; this mutation is commonly found in human B-ALL patients (Churchman *et al.* 2018).

Interestingly, JAK mutations were only observed in 3/7 control mice but were observed in 8/8 NAC-treated mice. Furthermore, the *Jak3* mutation was observed in all but two NAC mice, and these two mice were the two that harboured *Jak1* mutations. The mouse containing the M569K mutation located outside the pseudokinase domain also harboured the I741M mutation within the pseudokinase domain. In summary, 100% of NAC-treated mice had a mutation in the pseudokinase domain of either *Jak1* or *Jak3*, whereas only 3/7 control mice had pseudokinase JAK mutations. Previous work by our lab showed 12/19 untreated leukemias had at least one mutation in a *Jak1* or *Jak3* pseudokinase amino acid (Batista *et al.* 2018). This suggests that pseudokinase JAK mutations are not necessary for leukemogenesis in the Mb1-CreΔPB mouse model but may be necessary under treatment with NAC.

As mentioned briefly in the introduction, JAK/STAT signaling increases levels of intracellular ROS, which acts as a positive feedback loop to increase further JAK/STAT signaling (Prieto-Bermejo *et al.* 2018, Iiyama *et al.* 2006). Our lab has shown that administration of a JAK inhibitor Ruxolitinib decreases proliferation of Mb1-CreΔPB cells and reduced ROS and ROS-induced DNA damage in Mb1-CreΔPB mice. Lower levels of ROS due to NAC treatment may necessitate overactivation of JAK proteins to drive leukemia through pseudokinase mutations in the absence of normal JAK/STAT activation through ROS. Importantly none of the JAK mutations were C>A transversions

characteristic of ROS DNA damage, indicating that these mutations are created through alternate mechanisms present in both NAC-treated and control mice, such as AID activity. Whole exome sequencing or further analysis of the RNA sequencing data can clarify the proportion of total observed mutations that follow the C>A mutation characteristic of ROS damage.

4.7 Conclusion and hypothetical model

The initial hypothesis of this thesis was that high levels of ROS cause 8-oxoguanine DNA damage, leading to mutations that drive leukemic progression, and that this might be prevented by administration of the antioxidant N-acetylcysteine. From the data presented, we have shown that N-acetylcysteine does delay the initial onset of tumour growth but does not increase survival. Gene expression analysis suggests that the tumours that end up growing in the treated mice are more homogeneous, more aggressive, and therefore cause illness at a much faster rate once development has begun. This thesis discusses several possibilities for this outcome, however it is likely that the final consequence of N-acetylcysteine administration is impacted by a plethora of interconnecting pathways, as ROS are promiscuous in their signaling capabilities. It is thus very likely that multiple pathways including those examined in this thesis, plus more that have not yet been identified compound to result in the aggressive cancers seen in treatment mice. A working model that describes the cumulation of this thesis highlights the multitude of potential factors at play (**Figure 32**). The working hypothesis of the mechanism of NAC in our model of leukemia is that:

NAC tumours can evade cell death during early development through ROS-scavenging of NAC. This allows them to accumulate mutations in genes that work to drive leukemia, including those in *Jak1* and *Jak3*. Eventually, these mutations cumulate in a more aggressive leukemia that results in high levels of apoptotic signaling and fast onset of illness in Mb1-CreΔPB mice.

Altogether, the results discussed in this thesis demonstrate the importance of ROS signaling in both healthy immune function as well as cancer development and underscores the importance of driver mutations in the clonal evolution of cancer.

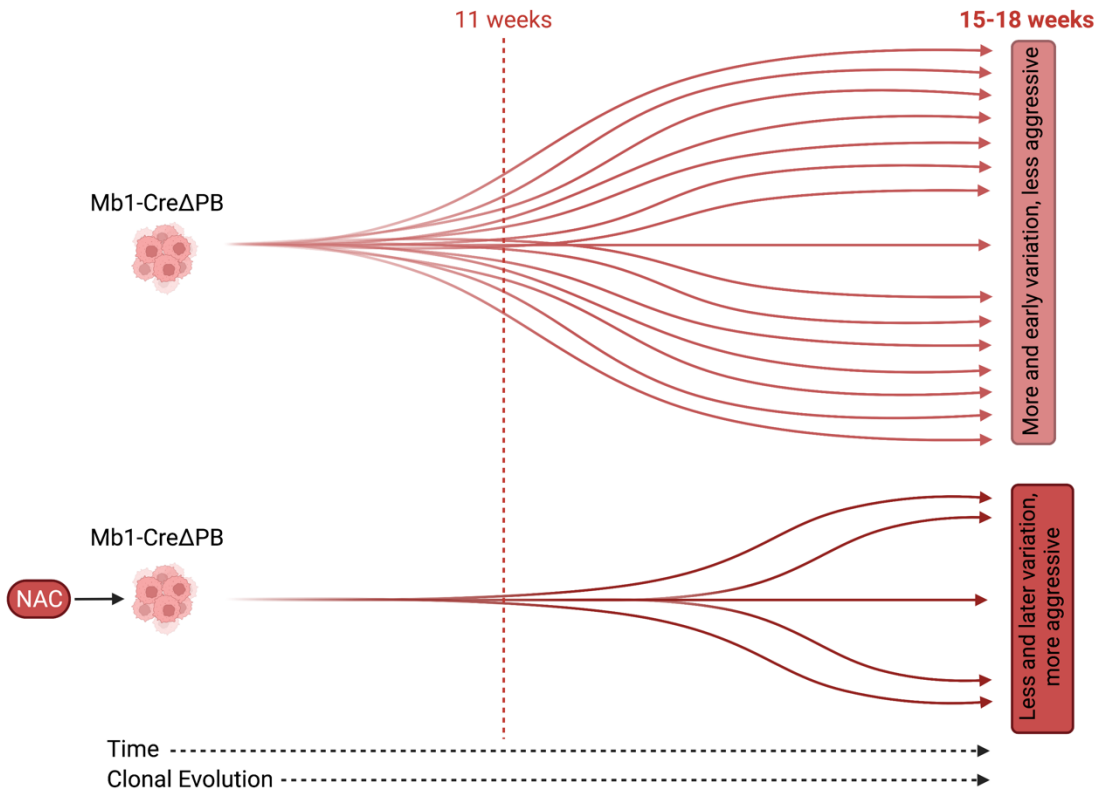

Figure 32. A working model of the process of 1g/L NAC delaying but streamlining leukemogenesis.

NAC tumours have less mutagenesis and therefore less tumour growth near the beginning of life, and thus by 11 weeks have small or undetectable tumour formation in the thymus. Control mice begin accumulation of mutations early on and thus by 11 weeks tend to have observable tumours. At some point between 11 weeks and time of euthanasia at roughly 15-18 weeks, NAC tumours begin developing mutations that act to significantly drive leukemia in a short period of time. These tumours are highly aggressive and fairly homogeneous. In contrast, control mice continue developing mutations, forming very heterogeneous tumours that eventually cause signs of illness at 15-18 weeks.

4.8 Future directions

Continuation of the heightened-dose NAC trials are ongoing to an endpoint of 15 mice in each group. These samples will also be submitted for RNA sequencing to determine if they follow the same pattern as the initial 1 g/L tumours or if they shed light on any new differentially expressed genes or recurrent mutations. Due to the nature of the results from the 11-week trial, we would like to repeat this with a variety of timepoints. Mice will be administered 1g/L NAC starting at week 3 and will be euthanized at weeks 5, 7, 9, 11, 13, and 15. Given that the overall median time to euthanasia is approximately 16 weeks, adding additional endpoints will give a broader picture of when leukemia begins to develop in control and treatment mice, and the length of time between a high CD19 positivity level and physical signs of sickness. This will hopefully provide more insight into how delayed tumour growth is in NAC-treated mice and how much faster the tumours progress to sickness. Additionally, treatment of Mb1-CreΔPB mice with a PI3K inhibitor may partially elucidate the mechanism behind which NAC tumours become more aggressive; if Mb1-CreΔPB mice survive longer when treated with PI3K inhibitors, this would suggest that increased activation of the PI3K pathway contributes to leukemogenesis. Dual treatment with NAC and PI3K would also provide interesting results if mice survive longer on both treatments versus NAC alone by blocking the overactivation of the PI3K pathway due to decreased PLC expression.

Whole exome sequencing of the 1g/L NAC tumour samples to further explore the mutational signatures, including frequency of C>A vs C>T mutations and identification of other highly mutated genes will be performed. This will also allow for genome-wide comparisons of overall frequency of mutagenesis and VAF measurements. Computational analysis of the mutation patterns may shed light on mechanisms of leukemogenesis that were not identified through the manual analysis of sequencing results performed here.

Further investigation into the gene expression analysis will hopefully give better insight into which pathways are affected by NAC and how these modifications translate into changes in how and when tumours develop. qPCR to confirm gene expression of selected

genes of interest will be performed, as well as Western blotting to investigate phosphorylation status of specific downstream elements of the pathways identified here.

We would also like to investigate the recurrent mutations discovered through RNA sequencing to determine if they are acting as drivers of leukemogenesis. We will double-infect bone marrow cells from Mb1-CreΔPB mice with lentiviral or retroviral vectors containing firefly luciferase and transplant these cells into immunodeficient mice. We will be able to visualize tumour growth *in vivo* using CT imaging technology and determine whether any of the mutations described here act to drive leukemia.

References

Agarwal, A., U. Muñoz-Nájar, U. Klueh, S.-C. Shih, and K. P. Claffey. 2004. N-acetyl-cysteine promotes angiostatin production and vascular collapse in an orthotopic model of breast cancer. *The American Journal of Pathology* 164: 1683–1696.

Andersen, S. 2004. Incorporation of dump into DNA is a major source of spontaneous DNA damage, while excision of uracil is not required for cytotoxicity of fluoropyrimidines in mouse embryonic fibroblasts. *Carcinogenesis* 26: 547–555.

Batista, C. R., M. Lim, A.-S. Laramée, F. Abu-Sardanah, L. S. Xu, R. Hossain, G. I. Bell, D. A. Hess, and R. P. DeKoter. 2018. Driver mutations in Janus kinases in a mouse model of B-cell leukemia induced by deletion of Pu.1 and SPI-B. *Blood Advances* 2: 2798–2810.

Batista, C. R., S. K. Li, L. S. Xu, L. A. Solomon, and R. P. DeKoter. 2017. Pu.1 regulates IG light chain transcription and rearrangement in pre-B cells during B cell development. *The Journal of Immunology* 198: 1565–1574.

Blanc, V., and N. O. Davidson. 2010. Apobec-1-mediated RNA editing. *WIREs Systems Biology and Medicine* 2: 594–602.

Bourgeais, J., N. Ishac, M. Medrzycki, M. Brachet-Botineau, L. Desbourdes, V. Gouilleux-Gruart, E. Pecnard, F. Rouleux-Bonnin, E. Gyan, J. Domenech, F. Mazurier, R. Moriggl, K. D. Bunting, O. Herault, and F. Gouilleux. 2016. Oncogenic STAT5 signaling promotes oxidative stress in chronic myeloid leukemia cells by repressing antioxidant defenses. *Oncotarget* 8: 41876–41889.

Brack, C., M. Hirama, R. Lenhard-Schuller, and S. Tonegawa. 1978. A complete immunoglobulin gene is created by somatic recombination. *Cell* 15: 1–14.

Casellas, R., U. Basu, W. T. Yewdell, J. Chaudhuri, D. F. Robbiani, and J. M. Di Noia. 2016. Mutations, kataegis and translocations in B cells: Understanding aid promiscuous activity. *Nature Reviews Immunology* 16: 164–176.

Chan, G. L., P. W. Doetsch, and W. A. Haseltine. 1985. Cyclobutane pyrimidine dimers and (6-4) photoproducts block polymerization by DNA polymerase I. *Biochemistry* 24: 5723–5728.

Churchman, M. L., M. Qian, G. te Kronnie, R. Zhang, W. Yang, H. Zhang, T. Lana, P. Tedrick, R. Baskin, K. Verbist, J. L. Peters, M. Devidas, E. Larsen, I. M. Moore, Z. Gu, C. Qu, H. Yoshihara, S. N. Porter, S. M. Pruett-Miller, G. Wu, E. Raetz, P. L. Martin, W. P. Bowman, N. Winick, E. Mardis, R. Fulton, M. Stanulla, W. E. Evans, M. V. Relling, C.-H. Pui, S. P. Hunger, M. L. Loh, R. Handgretinger, K. E.

Nichols, J. J. Yang, and C. G. Mullighan. 2018. Germline genetic IKZF1 variation and predisposition to childhood acute lymphoblastic leukemia. *Cancer Cell* 33: 937–938.

Clark, M. R., M. Mandal, K. Ochiai, and H. Singh. 2014. Orchestrating B cell lymphopoiesis through interplay of IL-7 receptor and pre-B cell receptor signalling. *Nature Reviews Immunology* 14: 69–80.

Conrad, C., Lymp, J., Thompson, V., Dunn, C., Davies, Z., Chatfield, B., Nichols, D., Clancy, J., Vender, R., Egan, M. E., Quittell, L., Michelson, P., Antony, V., Spahr, J., Rubenstein, R. C., Moss, R. B., Herzenberg, L. A., Goss, C. H., & Tirouvanziam, R. 2014. Long-term treatment with oral N-acetylcysteine: Affects lung function but not sputum inflammation in cystic fibrosis subjects. A phase II randomized placebo-controlled trial. *Journal of Cystic Fibrosis*, *14*(2), 219–227.

DeKoter, R. P., and P. J. Gibson. 2016. B cell leukemia and lymphoma. *Encyclopedia of Immunobiology* 279–286.

Desouky, O., N. Ding, and G. Zhou. 2015. Targeted and non-targeted effects of ionizing radiation. *Journal of Radiation Research and Applied Sciences* 8: 247–254.

Fillatreau, S., Sweenie, C. H., McGeachy, M. J., Gray, D., & Anderton, S. M. 2002. B cells regulate autoimmunity by provision of IL-10. *Nature Immunology*, *3*(10), 944–950.

Garrett-Sinha, L. A., G. H. Su, S. Rao, S. Kabak, Z. Hao, M. R. Clark, and M. C. Simon. 1999. Pu.1 and SPI-B are required for normal B cell receptor–mediated signal transduction. *Immunity* 10: 399–408.

Ghoreschi, K., A. Laurence, and J. J. O'Shea. 2009. Janus kinases in immune cell signaling. *Immunological Reviews* 228: 273–287.

Giloni, L., M. Takeshita, F. Johnson, C. Iden, and A. P. Grollman. 1981. Bleomycin-induced strand-scission of DNA. mechanism of deoxyribose cleavage. *Journal of Biological Chemistry* 256: 8608–8615.

Greaves, M., and C. C. Maley. 2012. Clonal Evolution in cancer. *Nature* 481: 306–313.

Hanahan, D. 2022. Hallmarks of cancer: New dimensions. *Cancer Discovery* 12: 31–46.

Hempel, N., and M. Trebak. 2017. Crosstalk between calcium and reactive oxygen species signaling in cancer. *Cell Calcium* 63: 70–96.

Henner, W. D., S. M. Grunberg, and W. A. Haseltine. 1982. Sites and structure of gamma radiation-induced DNA strand breaks. *Journal of Biological Chemistry* 257: 11750–11754.

Holmfeldt, L., L. Wei, E. Diaz-Flores, M. Walsh, J. Zhang, L. Ding, D. Payne-Turner, M. Churchman, A. Andersson, S.-C. Chen, K. McCastlain, J. Becksfort, J. Ma, G. Wu, S. N. Patel, S. L. Heatley, L. A. Phillips, G. Song, J. Easton, M. Parker, X. Chen, M. Rusch, K. Boggs, B. Vadodaria, E. Hedlund, C. Drenberg, S. Baker, D. Pei, C. Cheng, R. Huether, C. Lu, R. S. Fulton, L. L. Fulton, Y. Tabib, D. J. Dooling, K. Ochoa, M. Minden, I. D. Lewis, L. B. To, P. Marlton, A. W. Roberts, G. Raca, W. Stock, G. Neale, H. G. Drexler, R. A. Dickins, D. W. Ellison, S. A. Shurtleff, C.-H. Pui, R. C. Ribeiro, M. Devidas, A. J. Carroll, N. A. Heerema, B. Wood, M. J. Borowitz, J. M. Gastier-Foster, S. C. Raimondi, E. R. Mardis, R. K. Wilson, J. R. Downing, S. P. Hunger, M. L. Loh, and C. G. Mullighan. 2013. The genomic landscape of hypodiploid acute lymphoblastic leukemia. *Nature Genetics* 45: 242–252.

Iacobucci, I., and C. G. Mullighan. 2017. Genetic basis of acute lymphoblastic leukemia. *Journal of Clinical Oncology* 35: 975–983.

Iiyama, M., K. Kakihana, T. Kurosu, and O. Miura. 2006. Reactive oxygen species generated by hematopoietic cytokines play roles in activation of receptor-mediated signaling and in cell cycle progression. *Cellular Signalling* 18: 174–182.

Inoue, D., G.-L. Chew, B. Liu, B. C. Michel, J. Pangallo, A. R. D'Avino, T. Hitchman, K. North, S. C.-W. Lee, L. Bitner, A. Block, A. R. Moore, A. Yoshimi, L. Escobar-Hoyos, H. Cho, A. Penson, S. X. Lu, J. Taylor, Y. Chen, C. Kadoch, O. Abdel-Wahab, and R. K. Bradley. 2019. Spliceosomal disruption of the non-canonical BAF complex in cancer. *Nature* 574: 432–436.

Jacobs, A. L., and P. Schär. 2011. DNA glycosylases: In DNA repair and beyond. *Chromosoma* 121: 1–20.

Jacoby, E., Chien, C. D., & Fry, T. J. (2014). Murine models of acute leukemia: Important tools in current Pediatric Leukemia Research. *Frontiers in Oncology*, *4*, 95.

Jaramillo, M. C., and D. D. Zhang. 2013. The emerging role of the nrf2–KEAP1 signaling pathway in cancer. *Genes & Development* 27: 2179–2191.

Karim, F. D., L. D. Urness, C. S. Thummel, M. J. Klemsz, S. R. McKercher, A. Celada, C. Van Beveren, R. A. Maki, C. V. Gunther, and J. A. Nye. 1990. The ETS-domain: A new DNA-binding motif that recognizes a purine-rich core DNA sequence. *Genes & Development* 4: 1451–1453.

Kino, K., M. Hirao-Suzuki, M. Morikawa, A. Sakaga, and H. Miyazawa. 2017. Generation, repair and replication of guanine oxidation products. *Genes and Environment* 39: 21.

Klein, L., Kyewski, B., Allen, P. M., & Hogquist, K. A. (2014). Positive and negative selection of the T cell repertoire: What thymocytes see (and don't see). *Nature Reviews Immunology, 14*(6), 377–391.

Kunkel, T. A. 2009. Evolving views of DNA replication (in)fidelity. *Cold Spring Harbor Symposia on Quantitative Biology* 74: 91–101.

Kunkel, T. A. 2004. DNA replication fidelity. *Journal of Biological Chemistry* 279: 16895–16898.

Kwon, Y. 2021. Possible beneficial effects of N-acetylcysteine for treatment of triple-negative breast cancer. *Antioxidants*10: 169.

Laramée, A.-S., H. Raczkowski, P. Shao, C. Batista, D. Shukla, L. Xu, S. M. Haeryfar, Y. Tesfagiorgis, S. Kerfoot, and R. DeKoter. 2020. Opposing roles for the related ETS-family transcription factors SPI-B and SPI-C in regulating B cell differentiation and function. *Frontiers in Immunology* 11: 841.

Laurent, G., F. Solari, B. Mateescu, M. Karaca, J. Castel, B. Bourachot, C. Magnan, M. Billaud, and F. Mechta-Grigoriou. 2008. Oxidative stress contributes to aging by enhancing pancreatic angiogenesis and insulin signaling. *Cell Metabolism* 7: 113–124.

Lilljebjörn, H., M. Rissler, C. Lassen, J. Heldrup, M. Behrendtz, F. Mitelman, B. Johansson, and T. Fioretos. 2011. Whole-exome sequencing of Pediatric Acute Lymphoblastic Leukemia. *Leukemia* 26: 1602–1607.

Lim, M., C. R. Batista, B. R. de Oliveira, R. Creighton, J. Ferguson, K. Clemmer, D. Knight, J. Iansavitchous, D. Mahmood, M. Avino, and R. P. DeKoter. 2020. Janus kinase mutations in mice lacking PU.1 and SPI-B drive B cell leukemia through reactive oxygen species-induced DNA damage. *Molecular and Cellular Biology* 40.

Losdyck, E., T. Hornakova, L. Springuel, S. Degryse, O. Gielen, J. Cools, S. N. Constantinescu, E. Flex, M. Tartaglia, J.-C. Renauld, and L. Knoops. 2015. Distinct acute lymphoblastic leukemia (ALL)-associated Janus Kinase 3 (JAK3) mutants exhibit different cytokine-receptor requirements and JAK inhibitor specificities. *Journal of Biological Chemistry* 290: 29022–29034.

Madesh, M., and G. Hajnóczky. 2001. VDAC-dependent permeabilization of the outer mitochondrial membrane by superoxide induces rapid and massive cytochrome c release. *Journal of Cell Biology* 155: 1003–1016.

Morris, R., N. J. Kershaw, and J. J. Babon. 2018. The molecular details of cytokine signaling via the JAK/stat pathway. *Protein Science* 27: 1984–2009.

Mullighan, C. G., J. Zhang, R. C. Harvey, J. R. Collins-Underwood, B. A. Schulman, L. A. Phillips, S. K. Tasian, M. L. Loh, X. Su, W. Liu, M. Devidas, S. R. Atlas, I.-M. Chen, R. J. Clifford, D. S. Gerhard, W. L. Carroll, G. H. Reaman, M. Smith, J. R. Downing, S. P. Hunger, and C. L. Willman. 2009. Jak mutations in high-risk childhood acute lymphoblastic leukemia. *Proceedings of the National Academy of Sciences* 106: 9414–9418.

Mullighan, C. G., C. B. Miller, I. Radtke, L. A. Phillips, J. Dalton, J. Ma, D. White, T. P. Hughes, M. M. Le Beau, C.-H. Pui, M. V. Relling, S. A. Shurtleff, and J. R. Downing. 2008. BCR–ABL1 lymphoblastic leukaemia is characterized by the deletion of ikaros. *Nature* 453: 110–114.

Nunn, M. F., P. H. Seeburg, C. Moscovici, and P. H. Duesberg. 1983. Tripartite structure of the avian erythroblastosis virus E26 transforming gene. *Nature* 306: 391–395.

Nutt, S. L., and B. L. Kee. 2007. The transcriptional regulation of B cell lineage commitment. *Immunity* 26: 715–725.

Odell, I. D., S. S. Wallace, and D. S. Pederson. 2012. Rules of engagement for base excision repair in Chromatin. *Journal of Cellular Physiology* 228: 258–266.

Pinton, P., and R. Rizzuto. 2006. Bcl-2 and ca2+ homeostasis in the endoplasmic reticulum. *Cell Death & Differentiation*13: 1409–1418.

Prieto-Bermejo, R., M. Romo-González, A. Pérez-Fernández, C. Ijurko, and Á. Hernández-Hernández. 2018. Reactive oxygen species in haematopoiesis: Leukaemic cells take a walk on the Wild Side. *Journal of Experimental & Clinical Cancer Research* 37: 125.

Ray, P. D., B.-W. Huang, and Y. Tsuji. 2012. Reactive oxygen species (ROS) homeostasis and redox regulation in cellular signaling. *Cellular Signalling* 24: 981–990.

Rebollo, A., and C. Schmitt. 2003. Ikaros, Aiolos and Helios: Transcription regulators and lymphoid malignancies. *Immunology & Cell Biology* 81: 171–175.

Roberts, K. G., and C. G. Mullighan. 2015. Genomics in acute lymphoblastic leukaemia: Insights and treatment implications. *Nature Reviews Clinical Oncology* 12: 344–357.

Roberts, K. G., Y. Yang, D. Payne-Turner, W. Lin, J. K. Files, K. Dickerson, Z. Gu, J. Taunton, L. J. Janke, T. Chen, M. L. Loh, S. P. Hunger, and C. G. Mullighan. 2017. Oncogenic role and therapeutic targeting of ABL-class and JAK-STAT activating kinase alterations in Ph-like ALL. *Blood Advances*. 1:1657-1671.

Ron, Y., De Baetselier, P., Gordon, J., Feldman, M., & Segal, S. 1981. Defective induction of antigen-reactive proliferating T cells in B cell-deprived mice. *European Journal of Immunology*, *11*(12), 964–968.

Saharinen, P., and O. Silvennoinen. 2002. The pseudokinase domain is required for suppression of basal activity of JAK2 and JAK3 tyrosine kinases and for cytokine-inducible activation of signal transduction. *Journal of Biological Chemistry* 277: 47954–47963.

Scharer, O. D. 2013. Nucleotide excision repair in eukaryotes. *Cold Spring Harbor Perspectives in Biology* 5: a012609.

Schatz, D. G., M. A. Oettinger, and D. Baltimore. 1989. The V(D)J recombination activating gene, RAG-1. *Cell* 59: 1035–1048.

Schweitzer, B. L., K. J. Huang, M. B. Kamath, A. V. Emelyanov, B. K. Birshtein, and R. P. DeKoter. 2006. SPI-C has opposing effects to pu.1 on gene expression in progenitor B cells. *The Journal of Immunology* 177: 2195–2207.

Scott, L. M. 2013. Lymphoid malignancies: Another face to the Janus kinases. *Blood Reviews* 27: 63–70.

Scott, E. W., M. C. Simon, J. Anastasi, and H. Singh. 1994. Requirement of transcription factor PU.1 in the development of multiple hematopoietic lineages. *Science* 265: 1573–1577.

Shlomchik, M. J., and F. Weisel. 2012. Germinal center selection and the development of memory B and plasma cells. *Immunological Reviews* 247: 52–63.

Solomon, L. A., S. K. H. Li, J. Piskorz, L. S. Xu, and R. P. DeKoter. 2015. Genome-wide comparison of Pu.1 and SPI-B binding sites in a mouse B lymphoma cell line. *BMC Genomics* 16:76.

Swaminathan, S., L. Klemm, E. Park, E. Papaemmanuil, A. Ford, S.-M. Kweon, D. Trageser, B. Hasselfeld, N. Henke, J. Mooster, H. Geng, K. Schwarz, S. C. Kogan, R. Casellas, D. G. Schatz, M. R. Lieber, M. F. Greaves, and M. Müschen. 2015. Mechanisms of clonal evolution in Childhood Acute Lymphoblastic Leukemia. *Nature Immunology*16: 766–774.

Vazquez, M. I., Catalan-Dibene, J., & Zlotnik, A. 2015. B cells responses and cytokine production are regulated by their immune microenvironment. *Cytokine*, *74*(2), 318–326.

Viguera, E. 2001. Replication slippage involves DNA polymerase pausing and dissociation. *The EMBO Journal* 20: 2587–2595.

Wu, X., J. Feng, A. Komori, E. C. Kim, H. Zan, and P. Casali. 2003. Immunoglobulin Somatic Hypermutation: Double-Strand DNA Breaks, AID and Error-Prone DNA Repair. *Journal of Clinical Immunology* 23: 235–246.

Xu, L. S., K. M. Sokalski, K. Hotke, D. A. Christie, O. Zarnett, J. Piskorz, G. Thillainadesan, J. Torchia, and R. P. DeKoter. 2012. Regulation of B cell linker protein transcription by PU.1 and SPI-B in murine B cell acute lymphoblastic leukemia. *The Journal of Immunology* 189: 3347–3354.

Zhang, J., C. G. Mullighan, R. C. Harvey, G. Wu, X. Chen, M. Edmonson, K. H. Buetow, W. L. Carroll, I.-M. Chen, M. Devidas, D. S. Gerhard, M. L. Loh, G. H. Reaman, M. V. Relling, B. M. Camitta, W. P. Bowman, M. A. Smith, C. L. Willman, J. R. Downing, and S. P. Hunger. 2011. Key pathways are frequently mutated in high-risk childhood acute lymphoblastic leukemia: A report from the Children's Oncology Group. *Blood* 118: 3080–3087.

Zhang, X., Rastogi, P., Shah, B., & Zhang, L. 2017. B lymphoblastic leukemia/lymphoma: New insights into genetics, molecular aberrations, subclassification and targeted therapy. *Oncotarget*, *8*(39), 66728–66741.

Curriculum Vitae

Name:	Mia Sams
Post-secondary Education and Degrees:	University of Guelph Guelph, Ontario, Canada 2015-2020 B.Sc.Hons. Major in Biochemistry The University of Western Ontario London, Ontario, Canada 2020-2022 M.Sc In Progress Microbiology and Immunology
Honours and Awards:	Dean's Research Scholarship University of Western Ontario, $20,000 over 2 years 2021-2022 Second Place Oral Presentation at Child Health Research Day London, Ontario 2022
Related Work Experience	Teaching Assistant The University of Western Ontario 2021 Microbiology and Immunology 2500: Biology of Infection and Immunity 2022 Microbiology and Immunology 3620: Immunology Laboratory